پیـــرامون

استفاده از امواج مستقیم و بازتابی سامانه‌های ناوبری جهانی برای سنجش از دور اتمسفر و اقیانوس

مصـــطفی حســـینی

برگرفته از رساله دکتری زیر نظر:

پروفسور حسین نهاوندچی

سازمان نقشه‌برداری کشور، هفتم تیرماه ۱۴۰۱

On the Remote Sensing of the Atmosphere and Ocean Using Direct and Reflected GNSS Signals

Mostafa Hoseini

Supervisors:
Prof. Hossein Nahavandchi,
Prof. Jens Wickert,
Associate Prof. Egil Eide,
Prof. Ole Andersen

NTNU | Norwegian University of Science and Technology

May 27, 2022
Trondheim

Outline

- Introduction
- Motivation
- Conceptual Foundation
- Research Approach & Results
    1. GNSS-derived Tropospheric Data Products
    2. Ground-based GNSS-Reflectometry Measurements
    3. Spaceborne GNSS-Reflectometry Observations
- Concluding Remarks
- Outlook for Future Research

Introduction

Global Navigation Satellite Systems (GNSS)

- American GPS
  - 31 Satellites
- Russian GLONASS
  - 24 Satellites
- European Galileo
  - 24 Satellites
- Chinese BeiDou
  - 49 Satellites
- Japanese QZSS
  - 4 Satellites
- Indian IRNSS
  - 7 Satellites

*Number of current satellites in orbit are retrieved from: www.gnssplanning.com

GNSS applications

- Surveying & Mapping
- Navigation
- Timing
- Agriculture
- Mining Industry
- Geodynamics
- Marine
- Disaster management

GNSS for Remote Sensing

- Earth Observations
- Space Weather
- Environmental Monitoring

Geometry of the Signals

GNSS remote sensing measurements can be made based on two different geometries of the signals:

- **Direct signals**
- **Reflected signals**

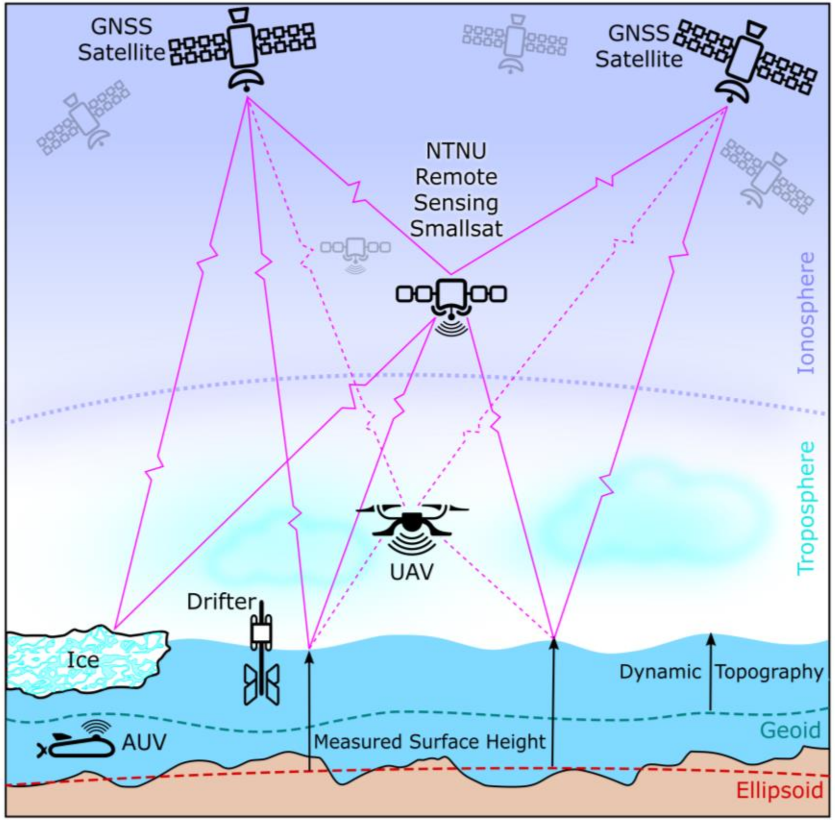

A Measuring Tool Beyond Expectations

- High precision
- High temporal resolution
- All-weather, day and night operation
- Low-demanding instrumentation
- Everywhere on or near Earth’s surface
- Long data archive for some applications

Motivation

Different Classes of GNSS Remote Sensing Data

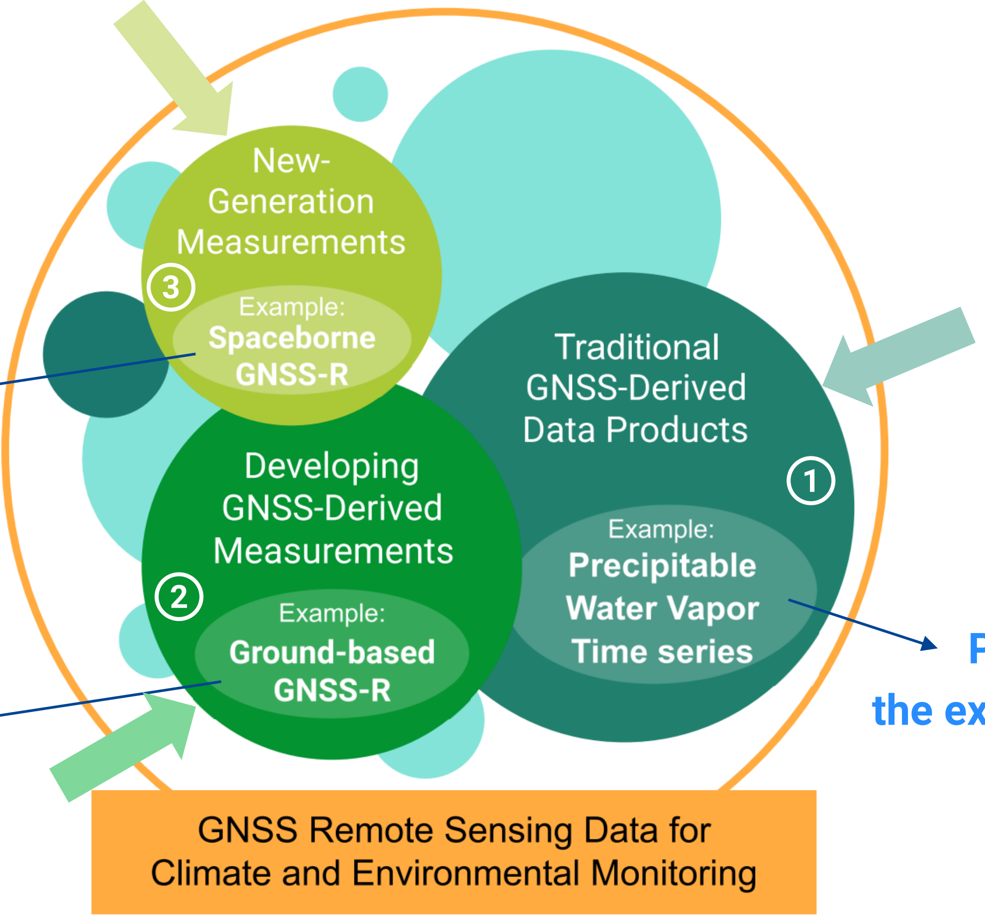

Demonstrating New applications

Quality Enhancement

Promoting the exploitation

Motivation

Conceptual Foundation

Conceptual Foundation

GNSS Signals

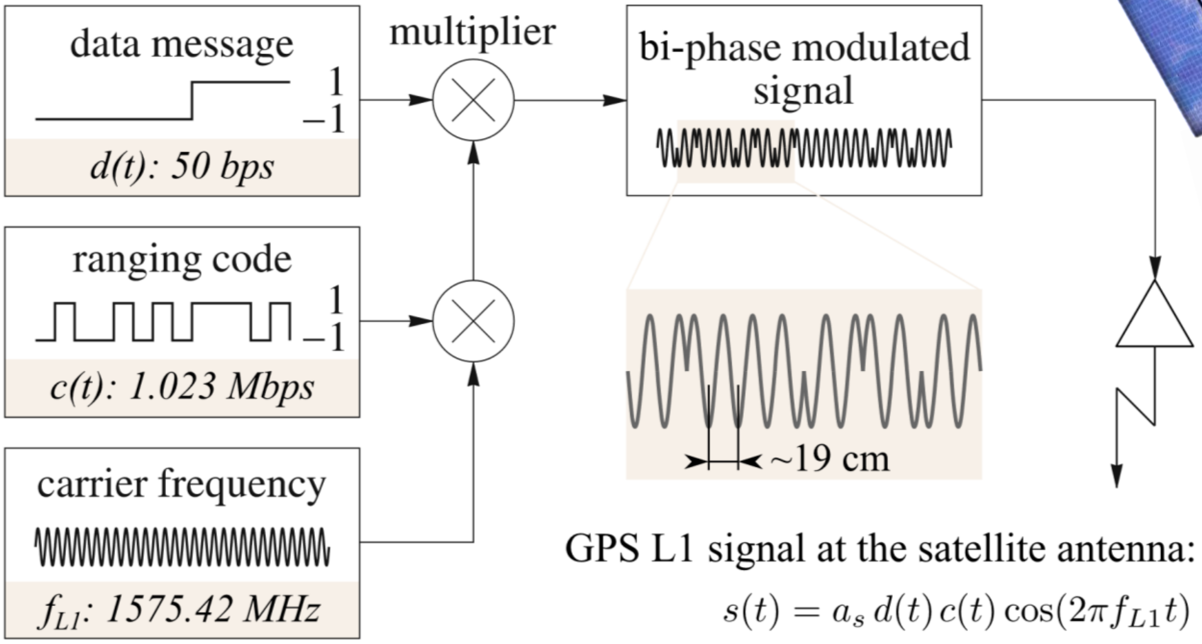

GPS L1 signal at the satellite antenna:

$$s(t) = a_s\, d(t)\, c(t) \cos(2\pi f_{L1} t)$$

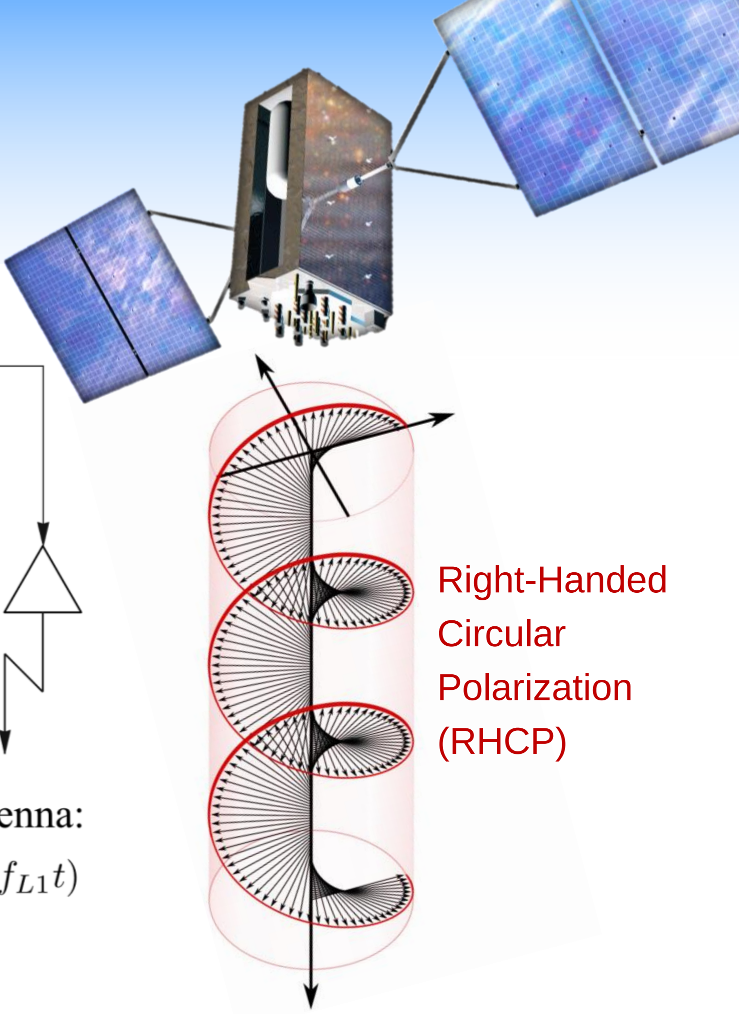

Right-Handed Circular Polarization (RHCP)

Conceptual Foundation

Reused from:
Hofmann-Wellenhof et al. (2008)

Delay-Doppler Map (DDM)

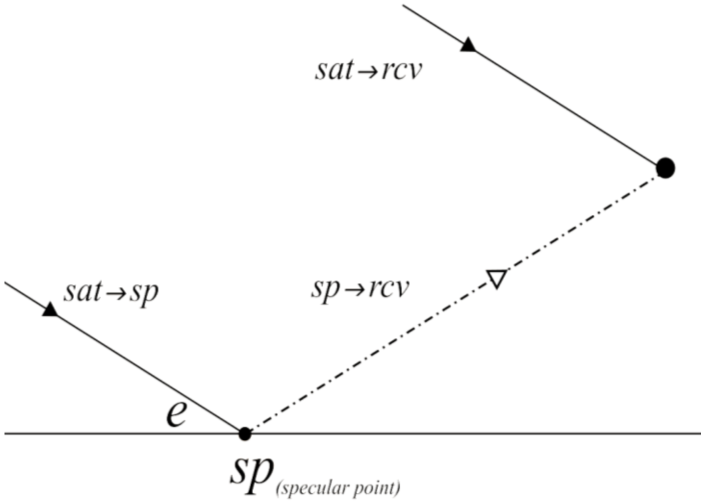

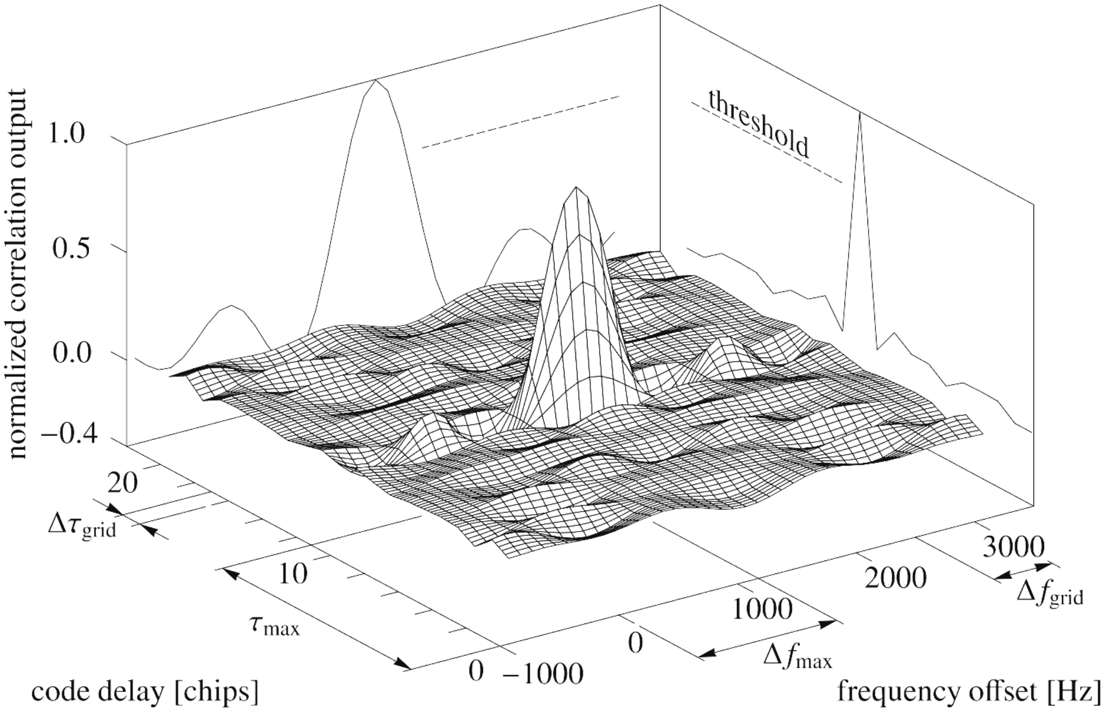

Hofmann-Wellenhof et al. (2008)

DDM for Reflected Signals

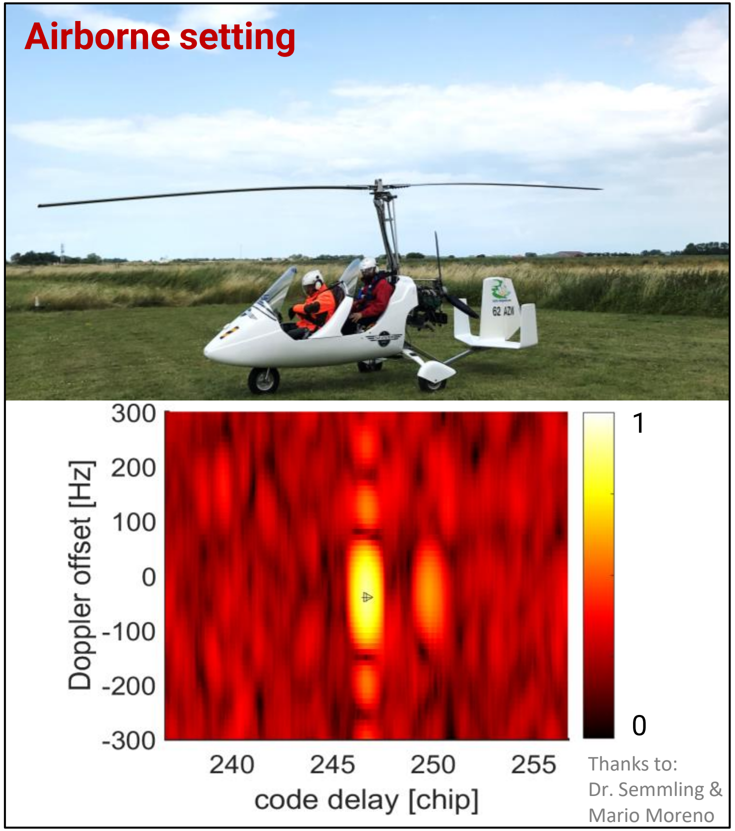

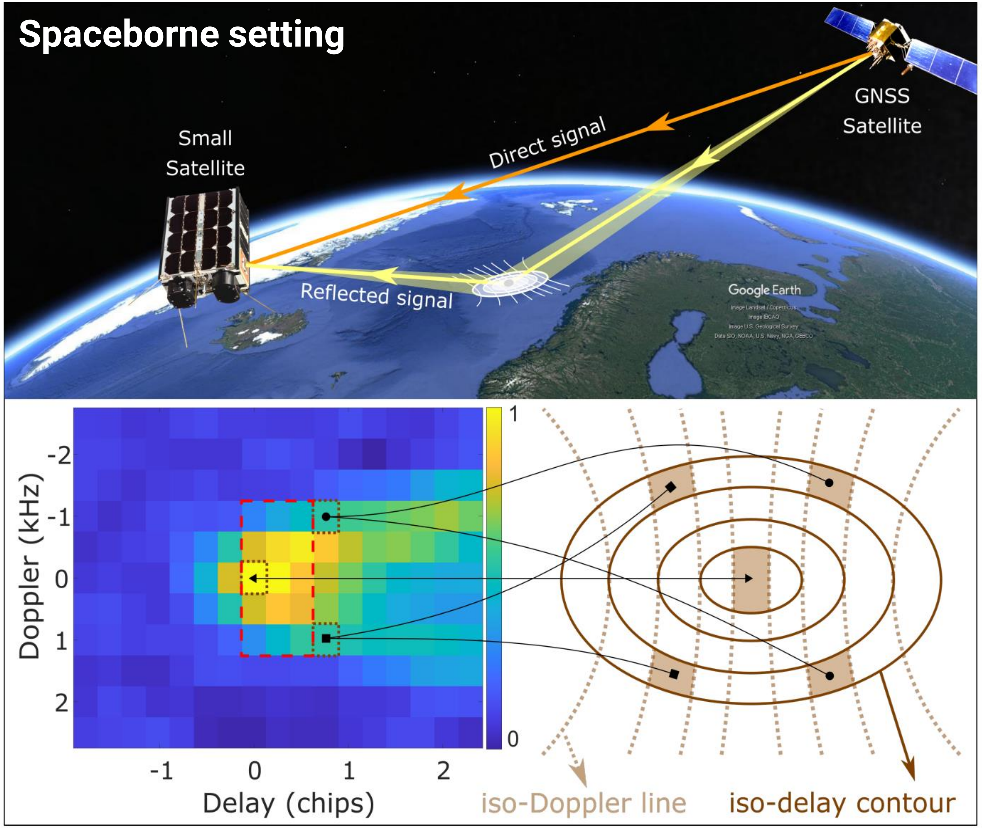

Primary Observables

- Delay of the signal
- Doppler frequency
- Carrier phase
- Estimate of signal strength

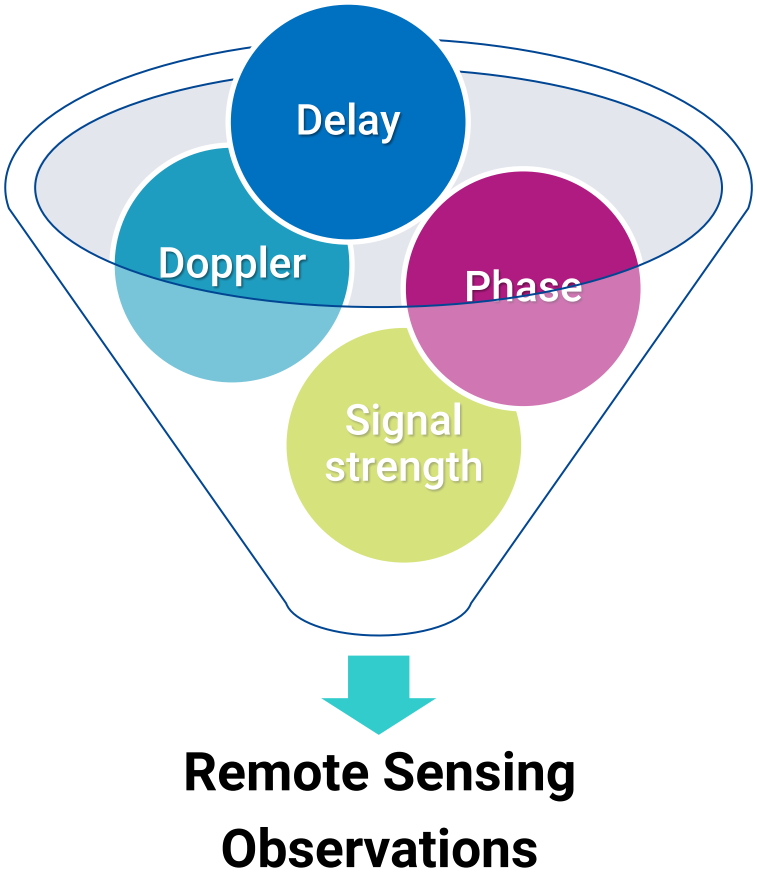

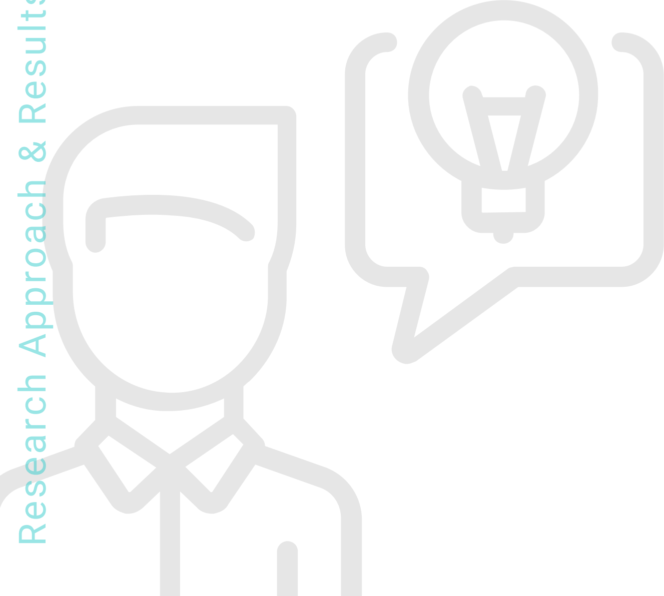

Research Approach & Results

Research Approach & Results

Research Approach

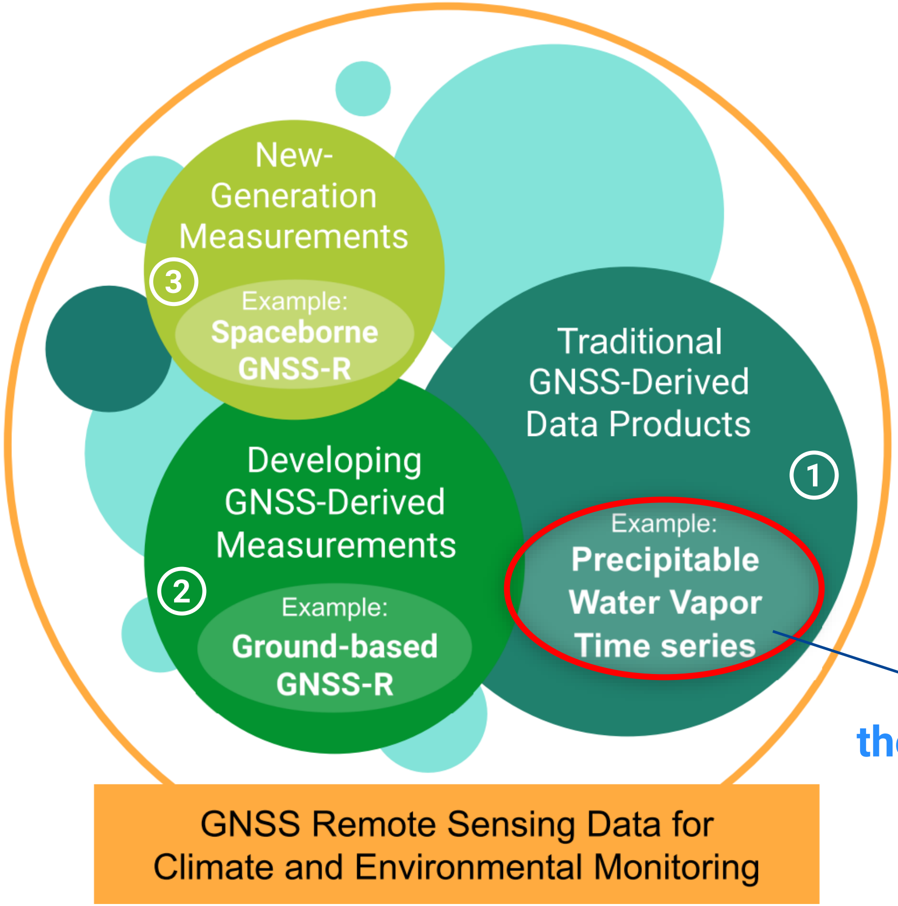

Promoting the exploitation

Research Approach & Results

1

GNSS-derived Tropospheric Data Products

(Precipitable Water Vapor)

GNSS-derived

Precipitable Water Vapor (PWV)

A traditional data product for the remote sensing of the troposphere using direct GNSS signals

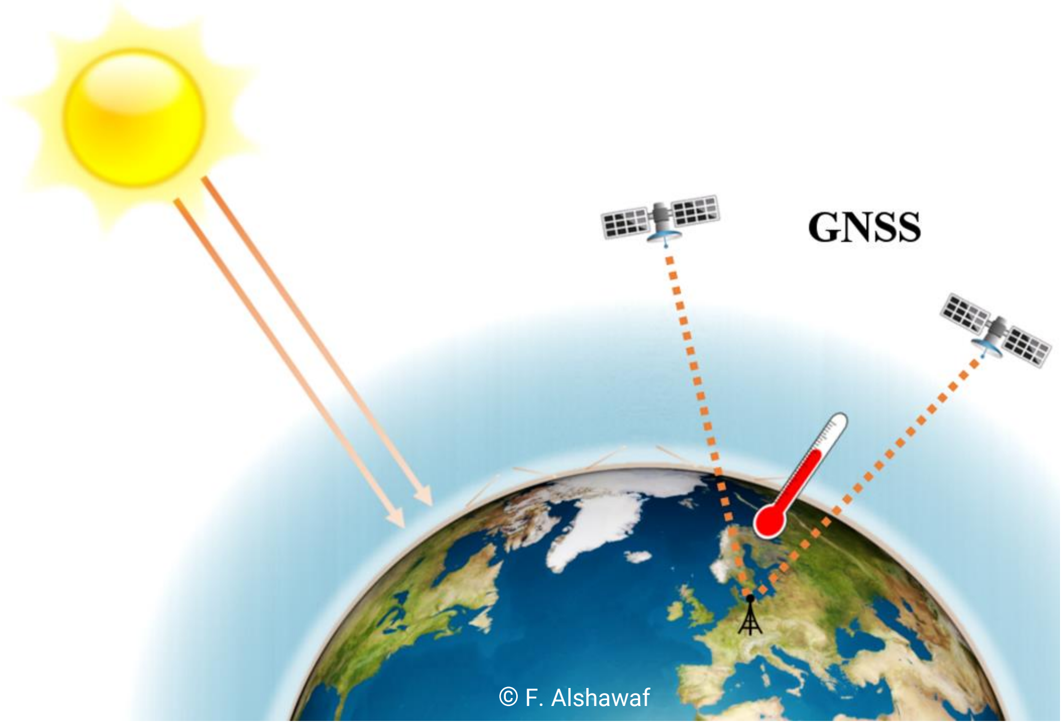

① # PWV for Climate Studies

- Model* data (1991–2015)
- 214 stations
- Positive water vapor trends
- Regional PWV patterns

***ERA-Interim**:

A global atmospheric data product

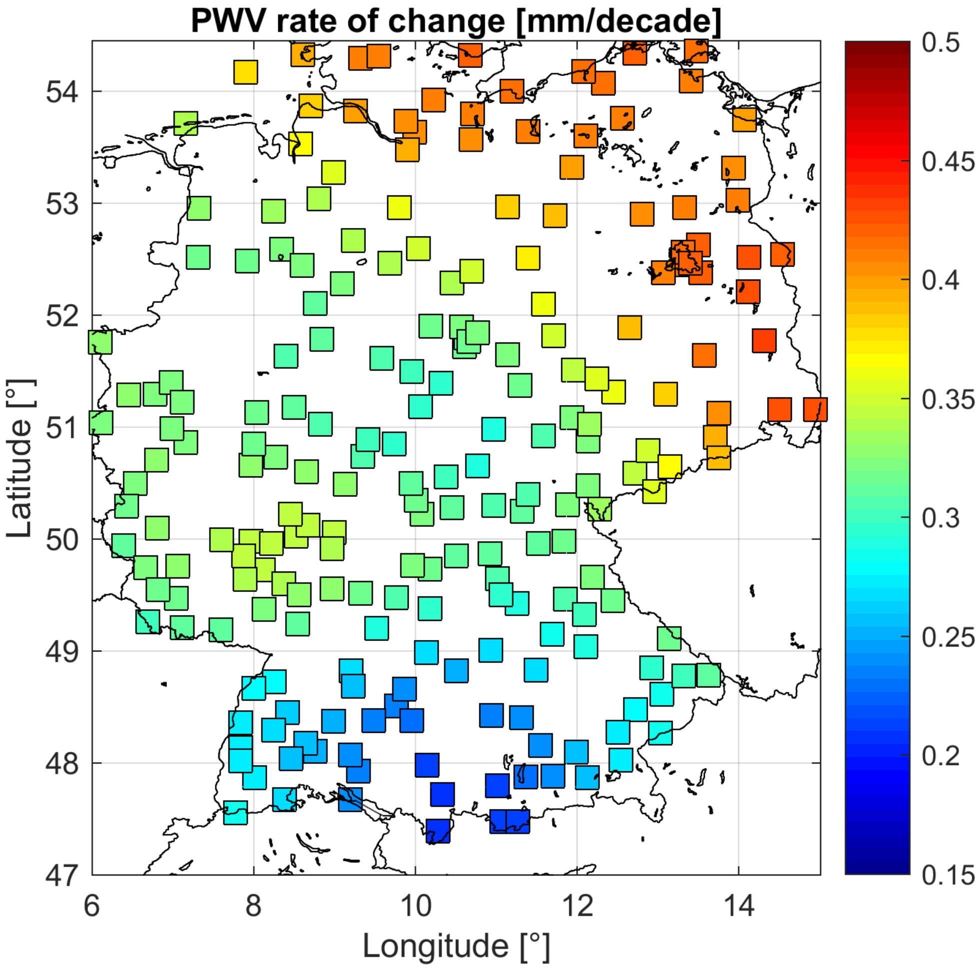

Research Approach & Results

① The Issue of Data Homogeneity

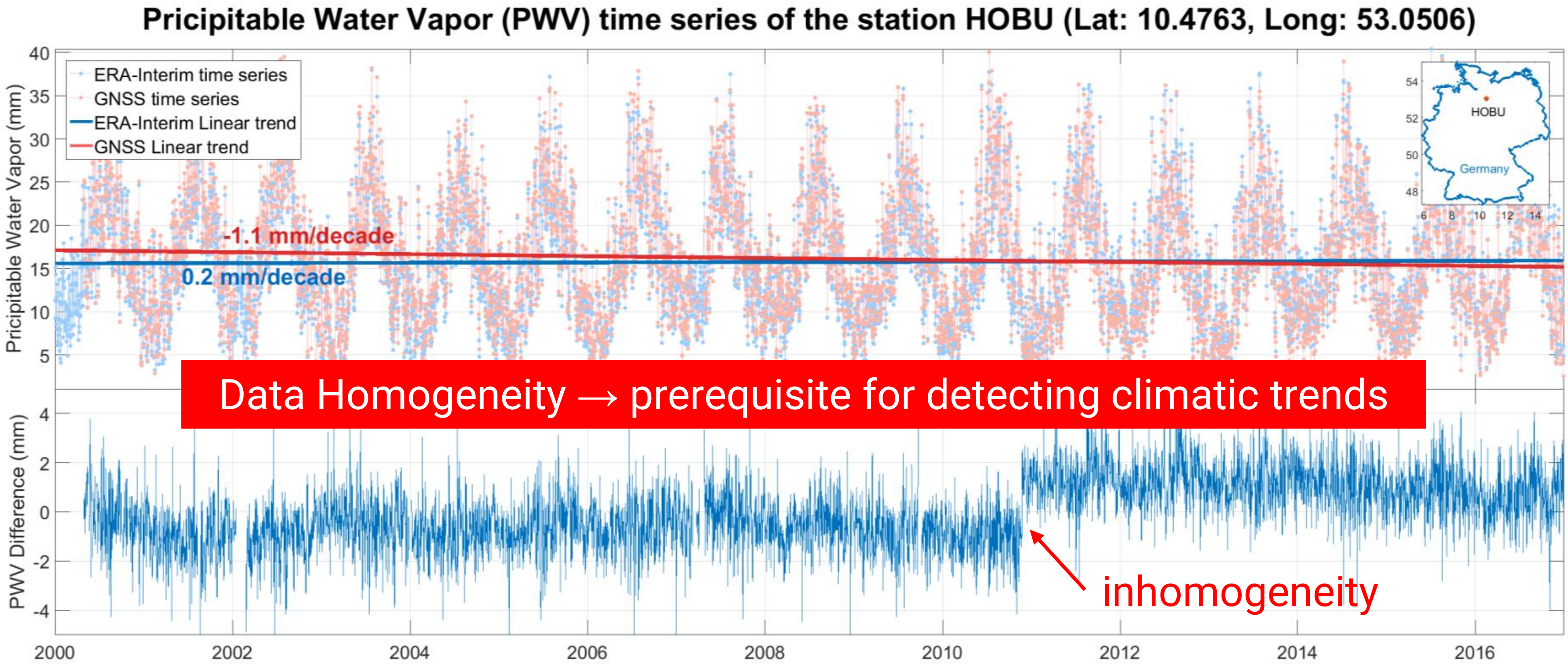

Data Homogeneity → prerequisite for detecting climatic trends

Research Approach & Results

NTNU

① A Novel Approach based on Singular Spectrum Analysis (SSA)

Zero-Difference Homogenization

- Independently applicable to each time series
- Leaves climate and meteorological signals unaffected

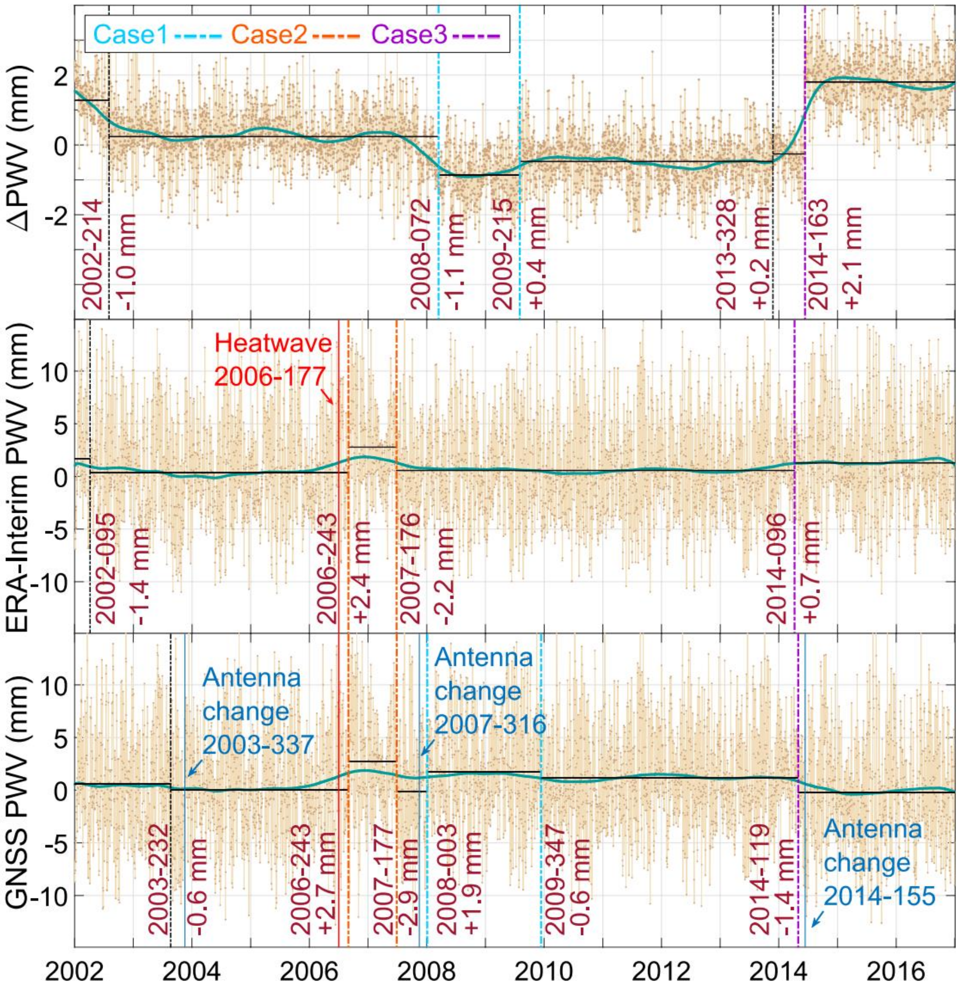

Hoseini M. et al. (2020)

① Impact of Homogenization

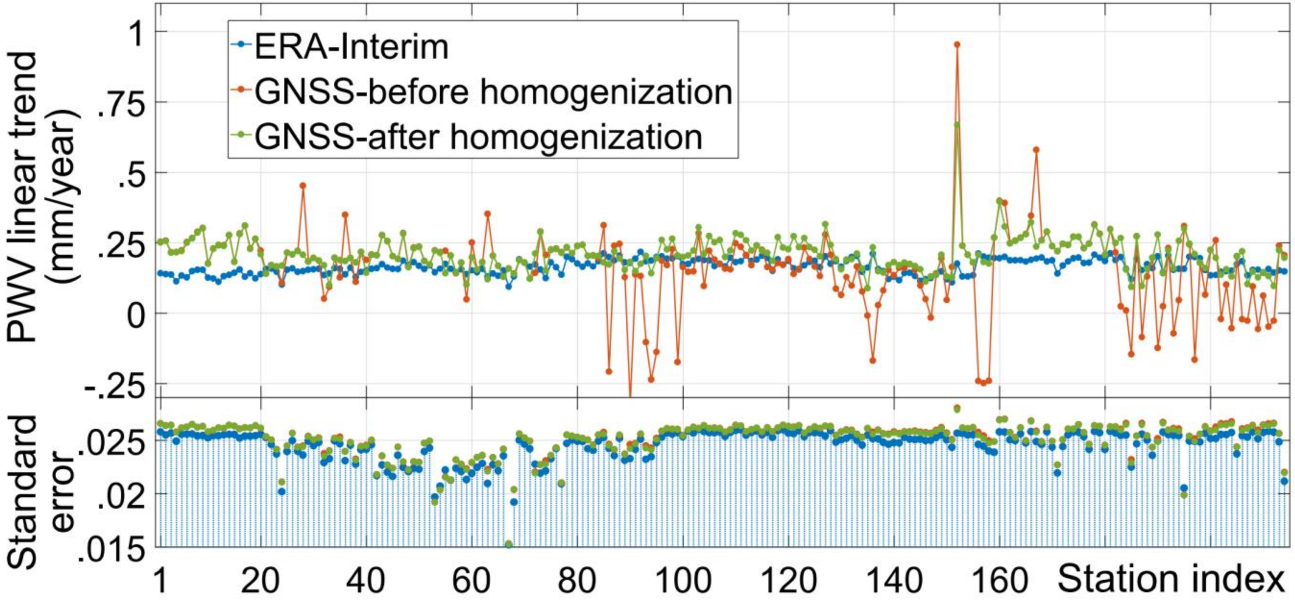

Summary for 214 GNSS stations over Germany	Difference	ERA-Interim	GNSS
Number of detected inhomogeneities	168	7	117
Detected undocumented changes	58	-	36

Hoseini M. et al. (2020)

Research Approach

Research Approach & Results

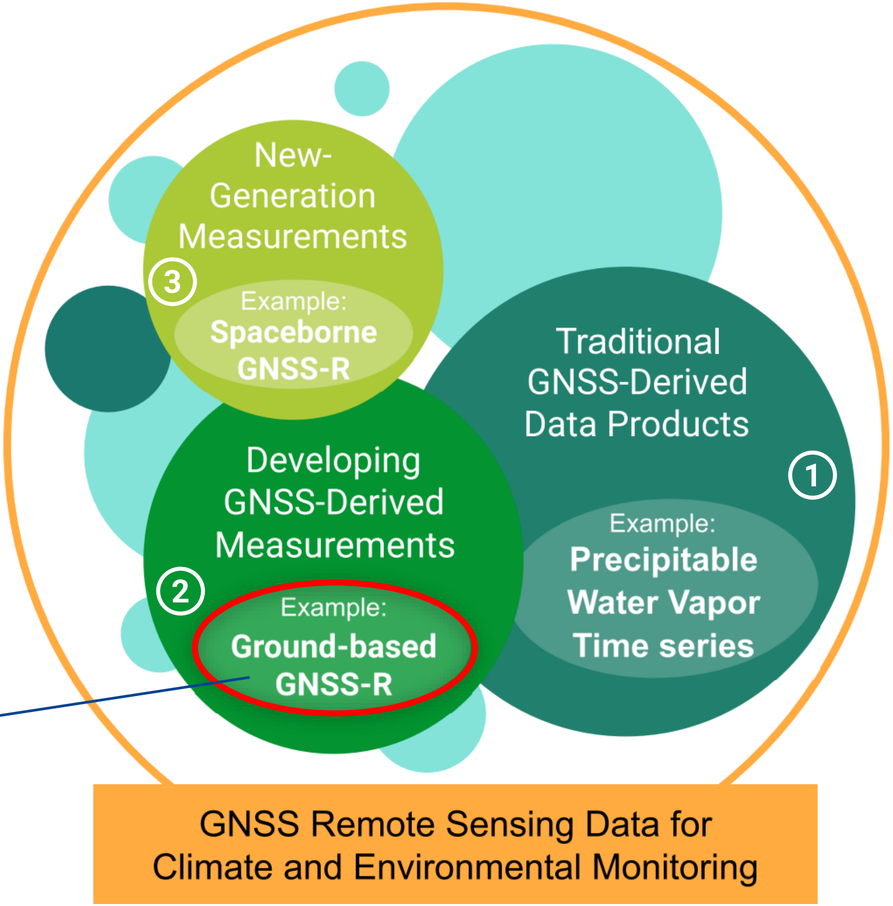

Quality Enhancement

Research Approach & Results

2

Ground-based GNSS-Reflectometry Measurements

(Sea Surface Characterization)

② A Dedicated GNSS-R Station

Installed and operated by:
German Research Center for Geosciences (GFZ)
Hosted by:
Onsala Space Observatory (OSO), Sweden

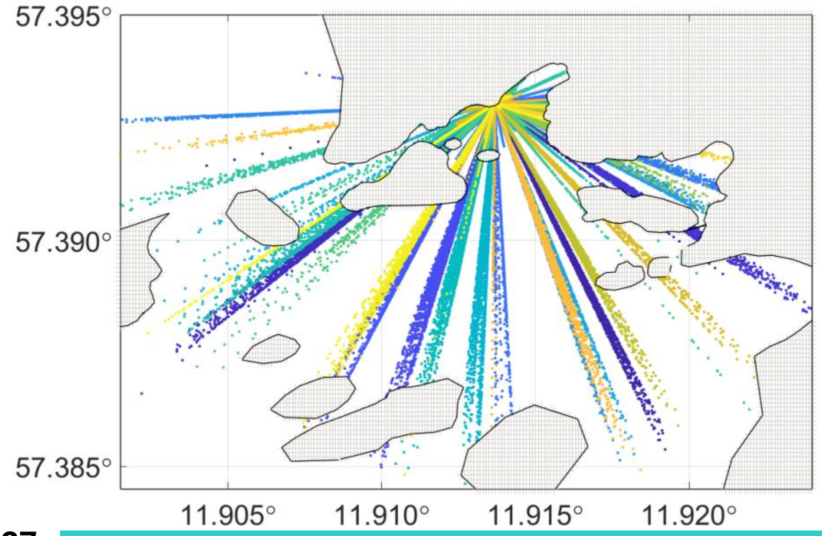

② GNSS-R Dataset Specifications

- From Jan. to Dec. **2016**
- Raw output at In-phase and Quadrature (**I/Q**) levels
- 200 Hz converted to **0.1 Hz**
- Two sea-looking antennas with **RHCP** and **LHCP**
- About **3 m** above sea level

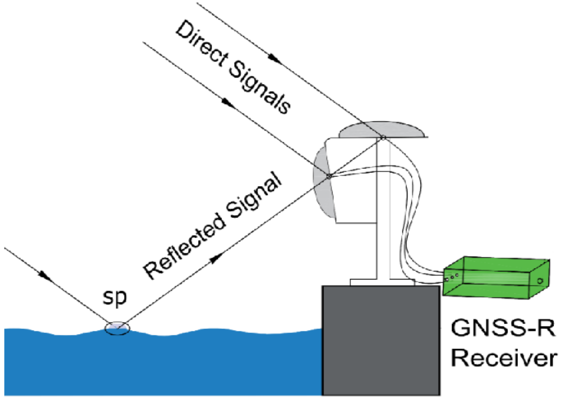

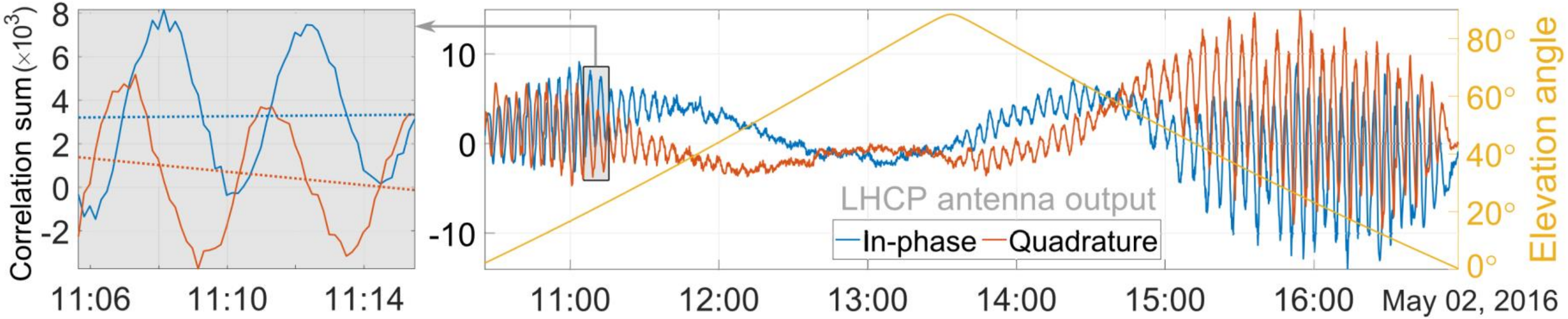

Research Approach & Results

Sea Surface Characterization using Ground-based GNSS-Reflectometry (GNSS-R)

- Estimation of **sea surface roughness** (sea state)
- Effect of **rainfall** on the sea surface
- **Sea-level** monitoring

Sea Surface Roughness

Hoseini et al. (2021)

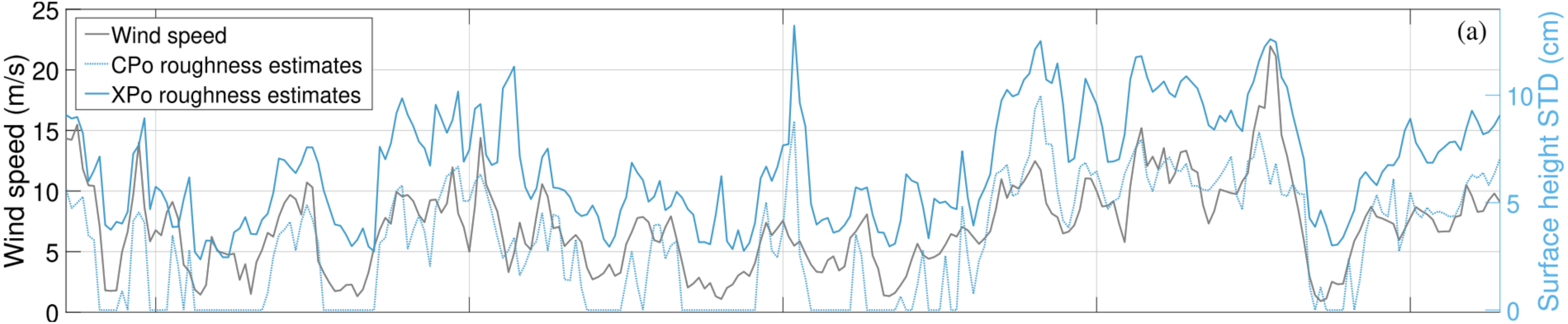

CPo: Co-Polarization antenna (RHCP)

XPo: Cross-Polarization antenna (LHCP)

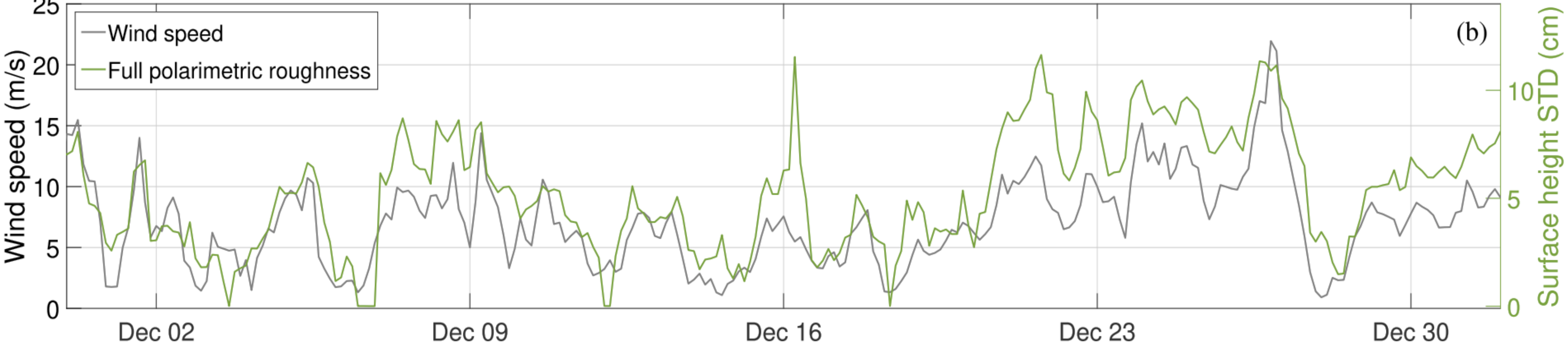

Research Approach & Results

2 Sea Surface Roughness

Hoseini et al. (2021)

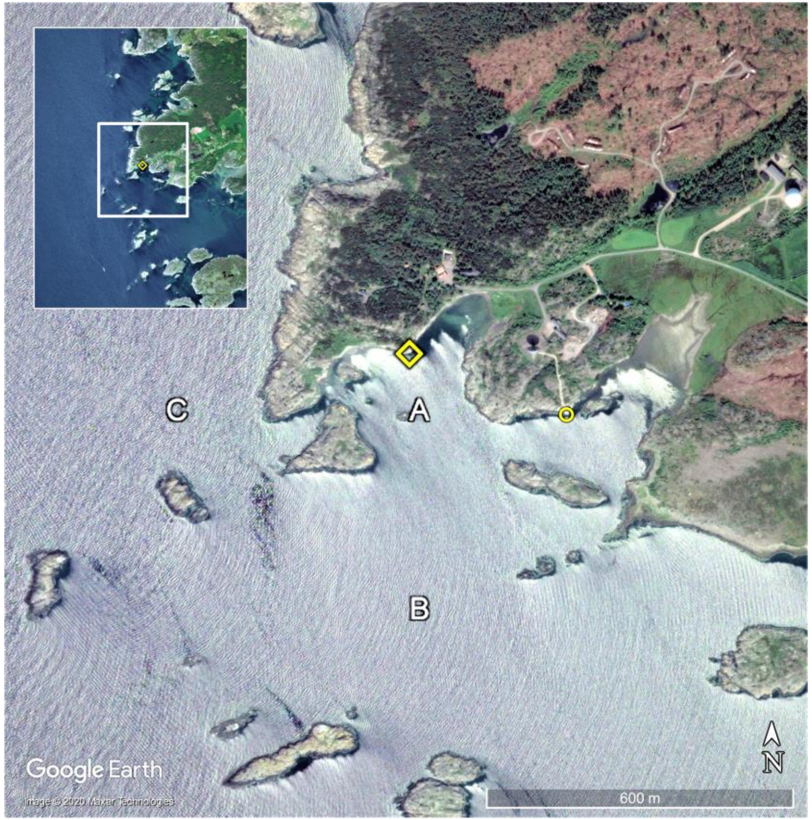

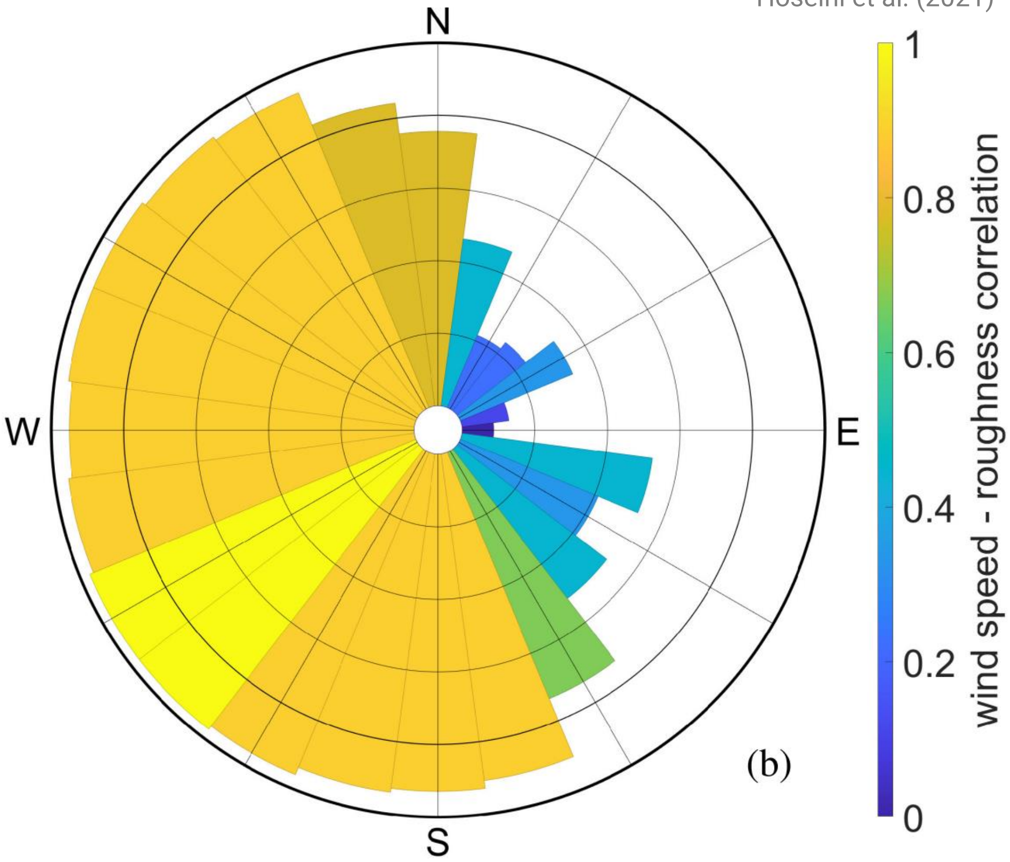

GNSS-R Response to Precipitation

Impact on the power of reflected signals

Sea-looking
RHCP Antenna

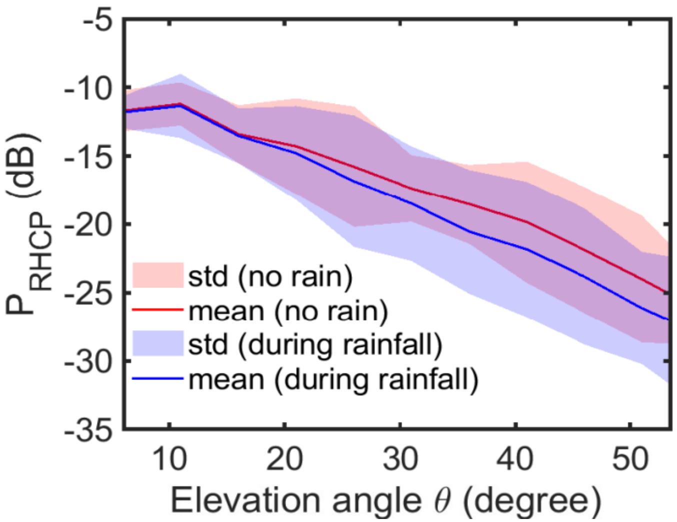

Sea-looking
LHCP Antenna

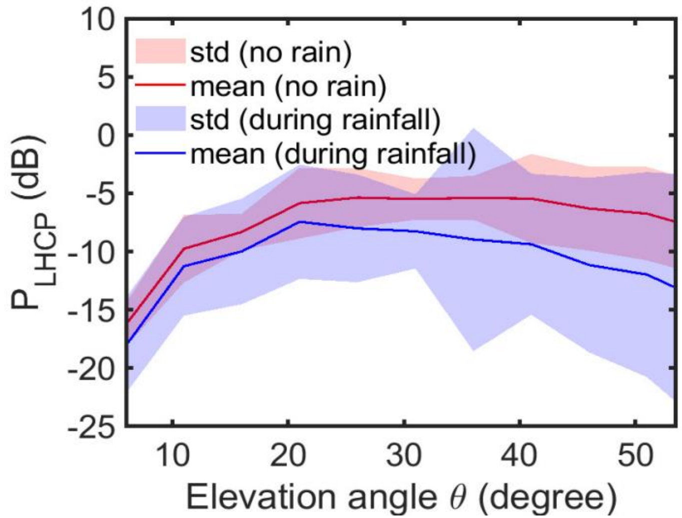

Asgarimehr M.,
Hoseini M., et al. (2021)

NTNU

② GNSS-R Response to Precipitation

Impact on the

Sea Surface Roughness (σ) and Sea Surface Salinity (SSS)

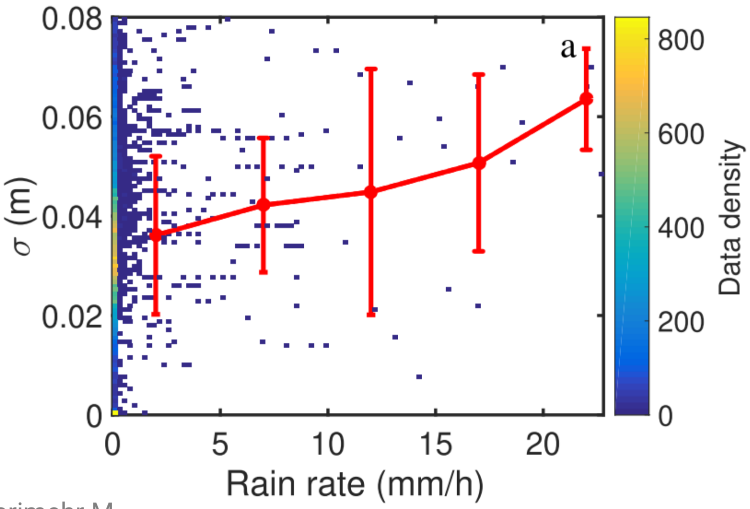

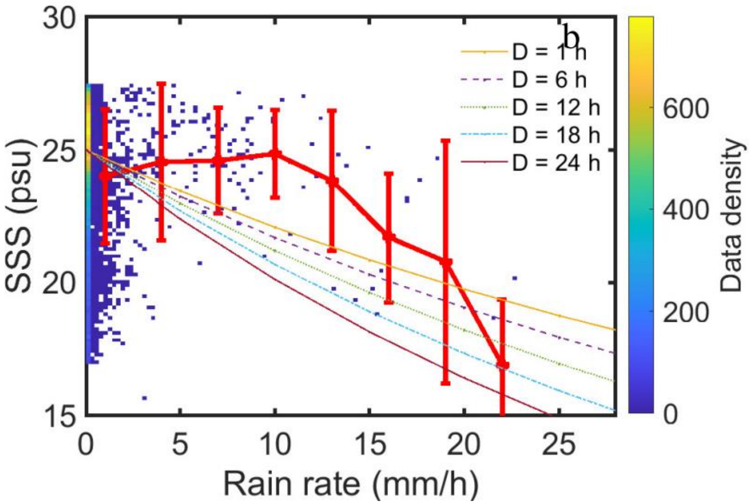

Asgarimehr M.,
Hoseini M., et al. (2021)

GNSS-R Sea Level Monitoring

Rajabi M., Hoseini M., et al. (2021)

Performance assessment under different scenarios

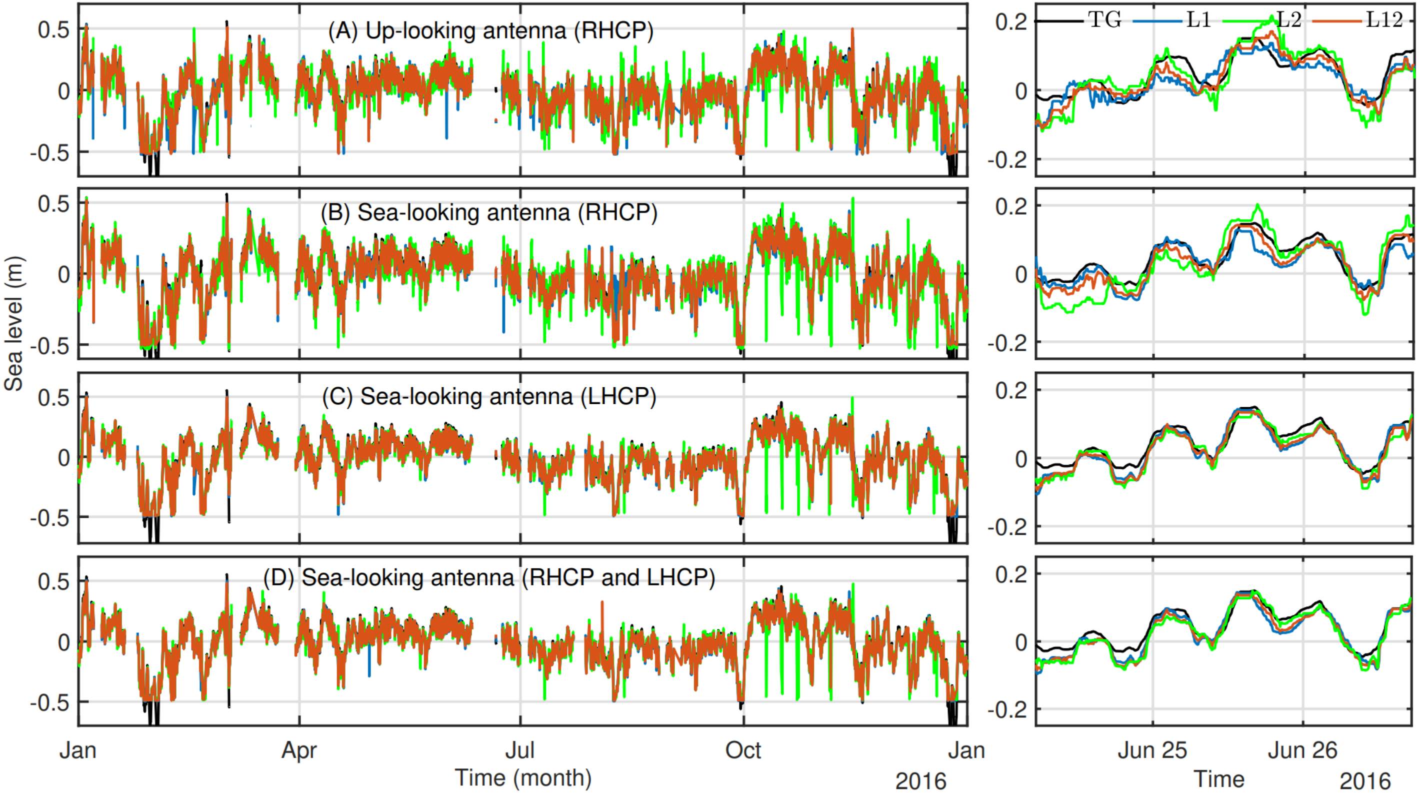

② GNSS-R Sea Level Monitoring

Combination of L1 and L2 = improvement up to about 25% and 40% w.r.t L1 and L2

Combined L1 & L2 results w.r.t the nearby tide gauge:

Scenario	RMSE (cm)	Corr (%)
A	4.1	96.9
B	3.1	98.2
C	2.4	99.0
D	2.3	99.0

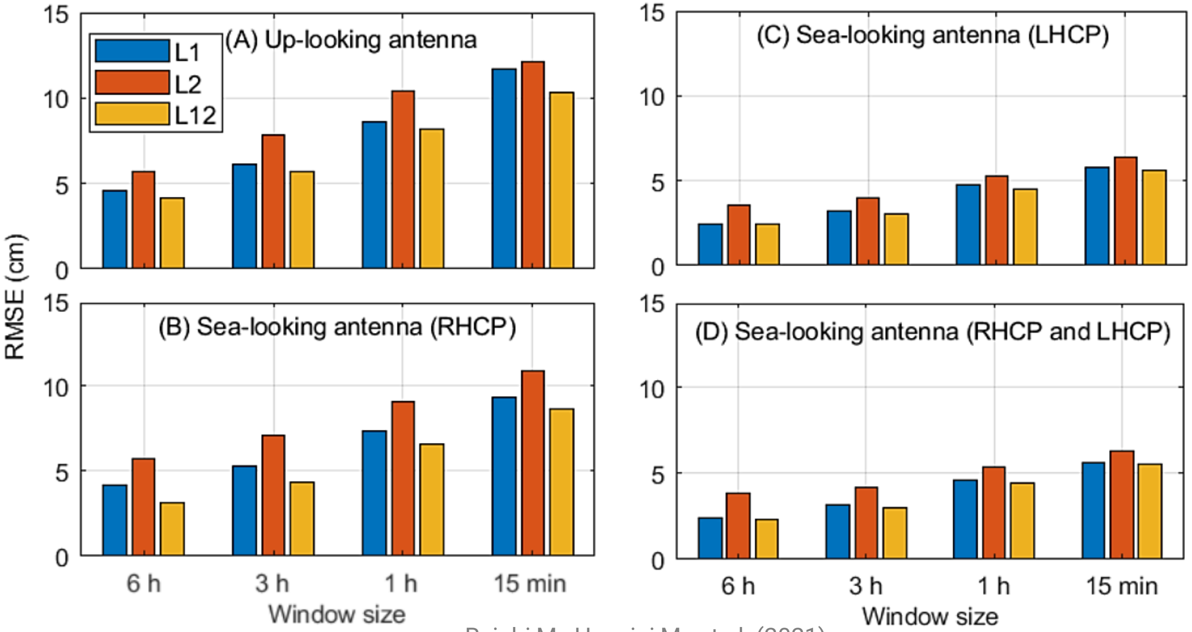

Rajabi M., Hoseini M., et al. (2021)

Research Approach & Results

GNSS-R Sea Level Monitoring

Performance under different sea states

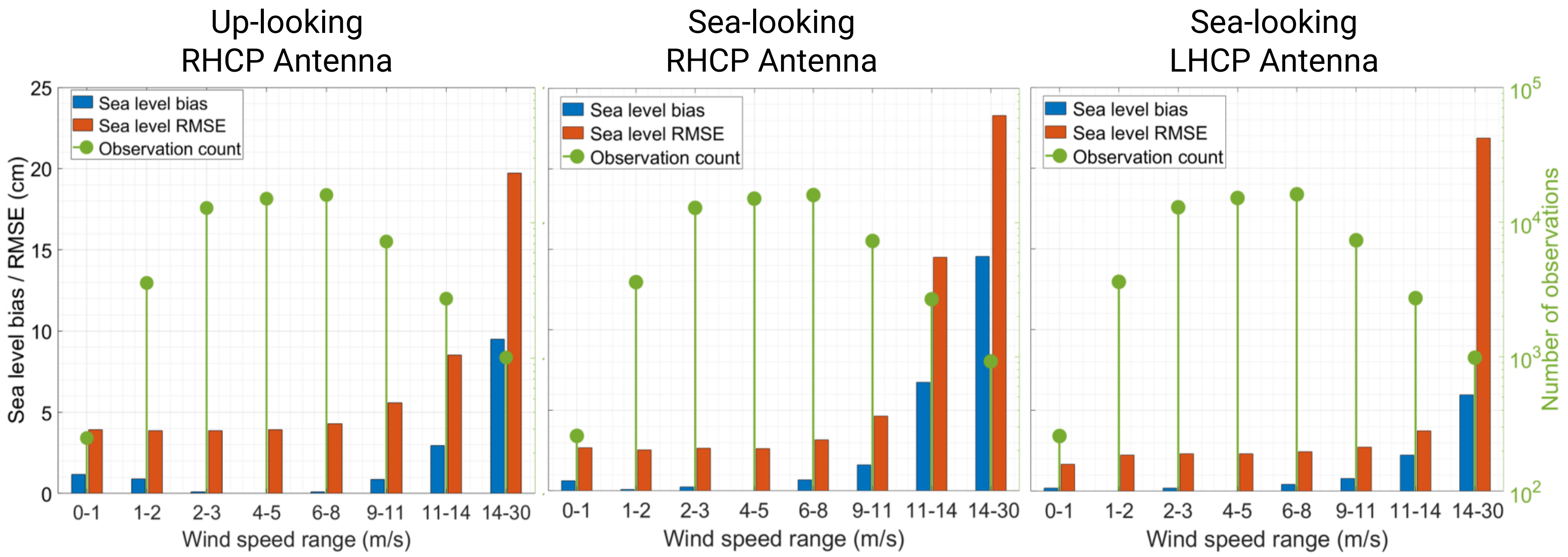

Rajabi M., Hoseini M., et al. (2021)

Research Approach & Results

NTNU

Research Approach

Demonstrating
New applications

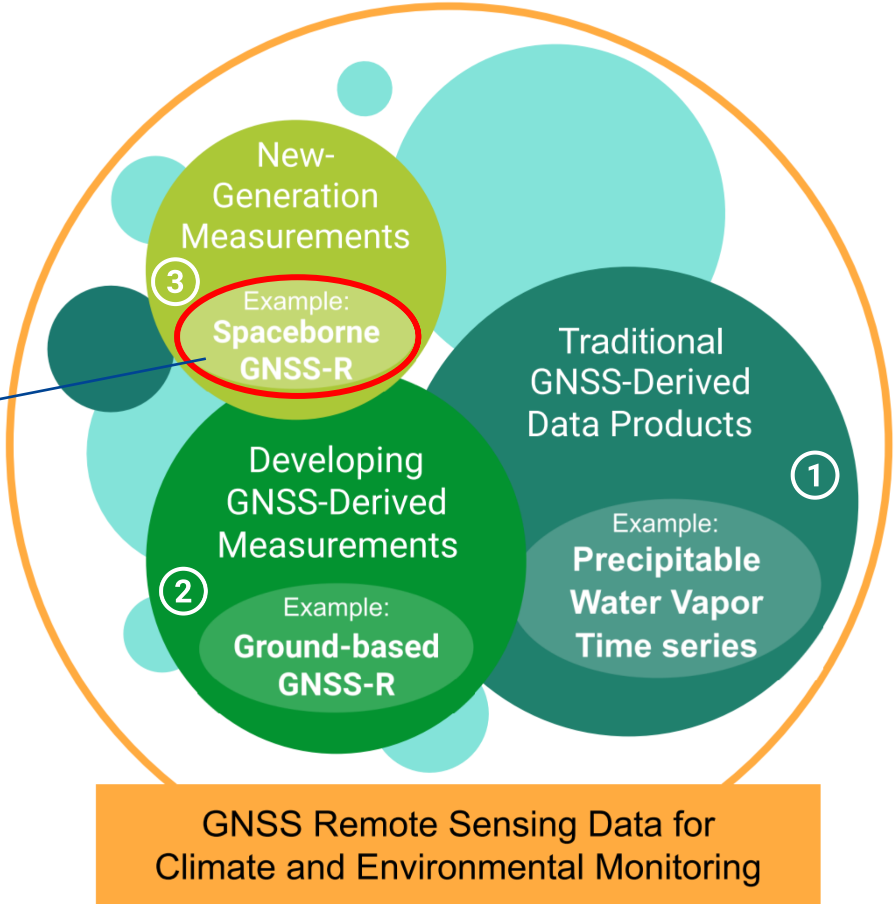

Research Approach & Results

3

Spaceborne GNSS-Reflectometry Observations

(Mesoscale Ocean Eddies, Floods)

Spaceborne GNSS-R Dataset

NASA Cyclone GNSS (CYGNSS)

- Constellation of 8 micro-satellites
- Altitude: ~520 km (LEO)
- Revisit time: ~7 hours
- Coverage: 38^{o}S - 38^{o}N latitudes

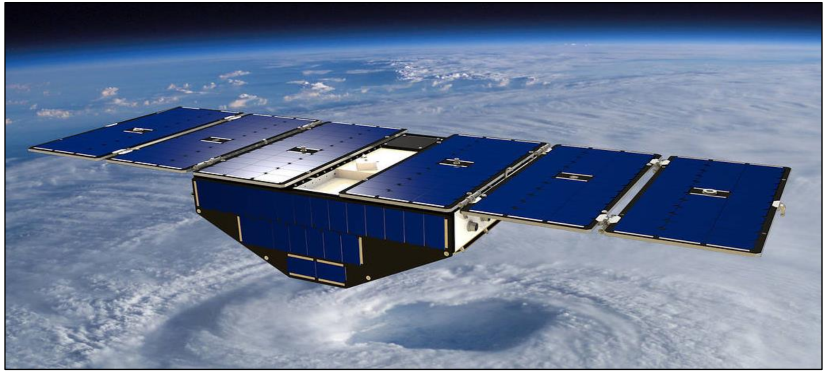

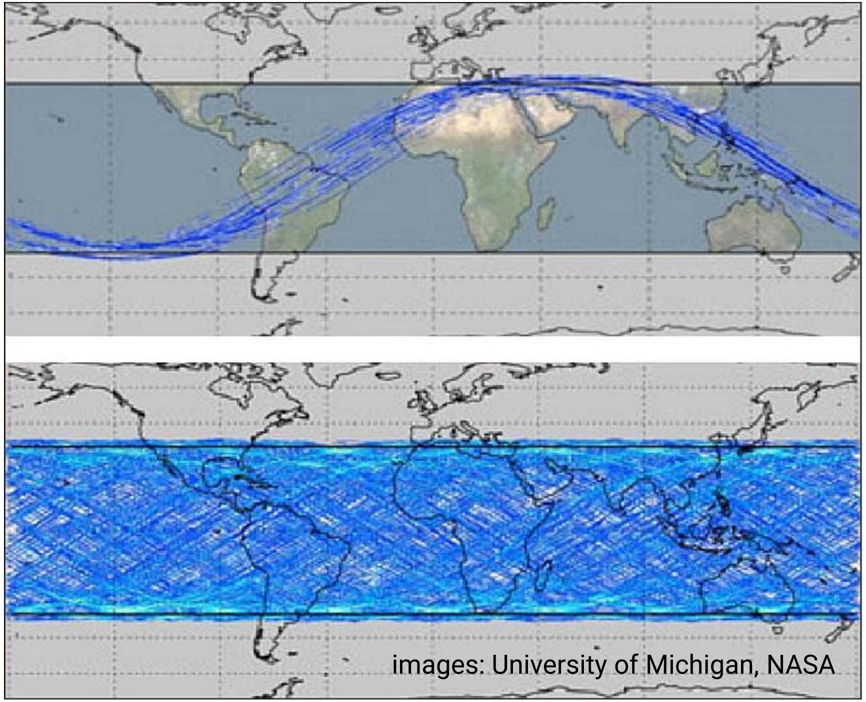

images: University of Michigan, NASA

3 Spaceborne GNSS-R Observations of

Mesoscale ocean eddies

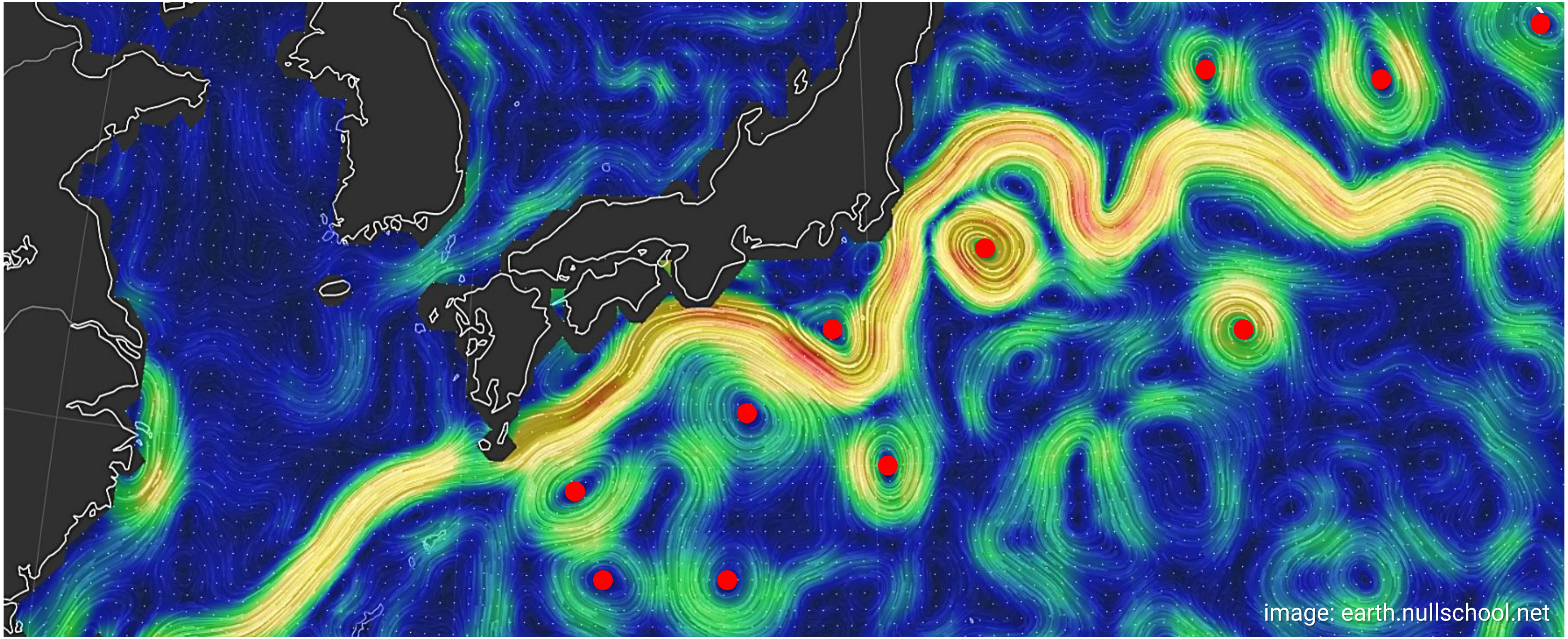

③ GNSS-R Response to the Ocean Eddies

For the first time, we reported on the feasibility of observing the oceanic eddies in spaceborne GNSS-R observations

Research Approach & Results

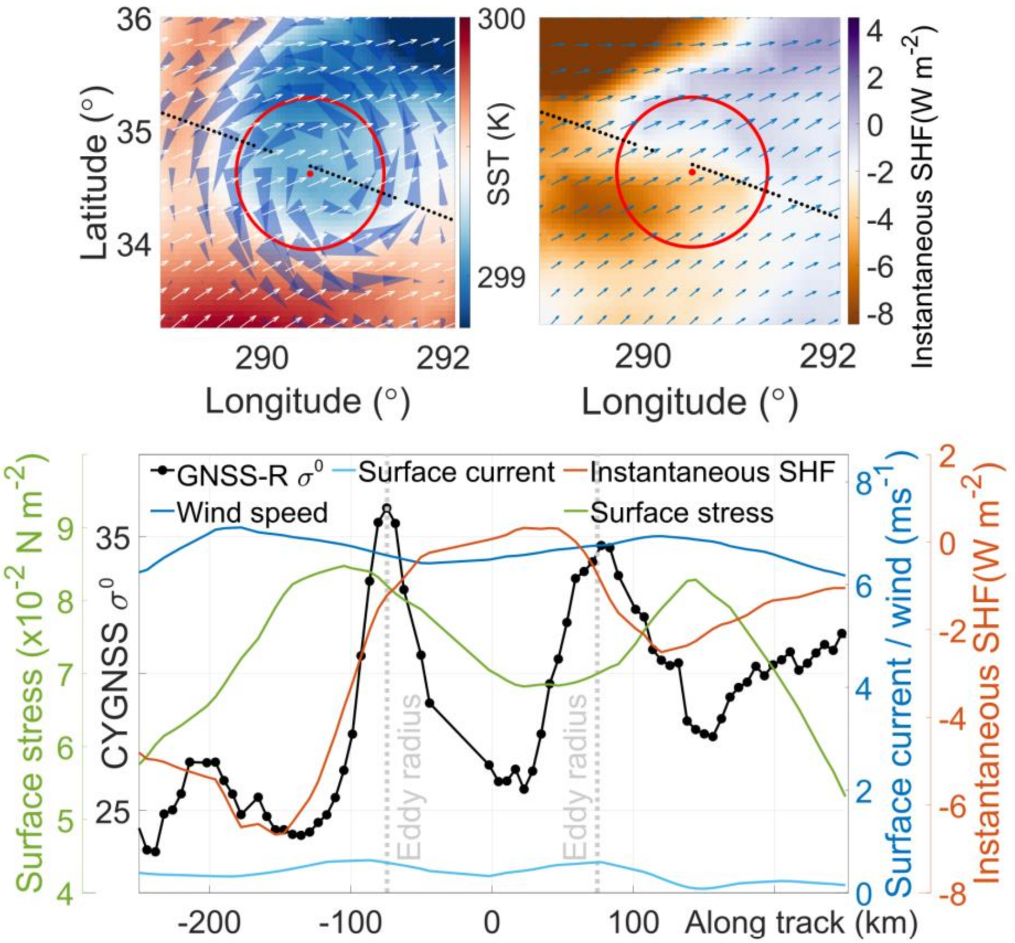

Hoseini M. et al. (2020)

NTNU

Spaceborne GNSS-R Observations of
Flooding Events

③ GNSS-R Response to Floods

Research Approach & Results

Published in Water (2020)

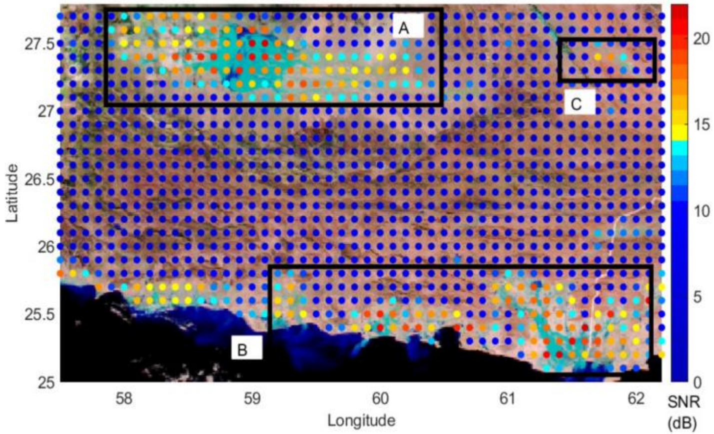

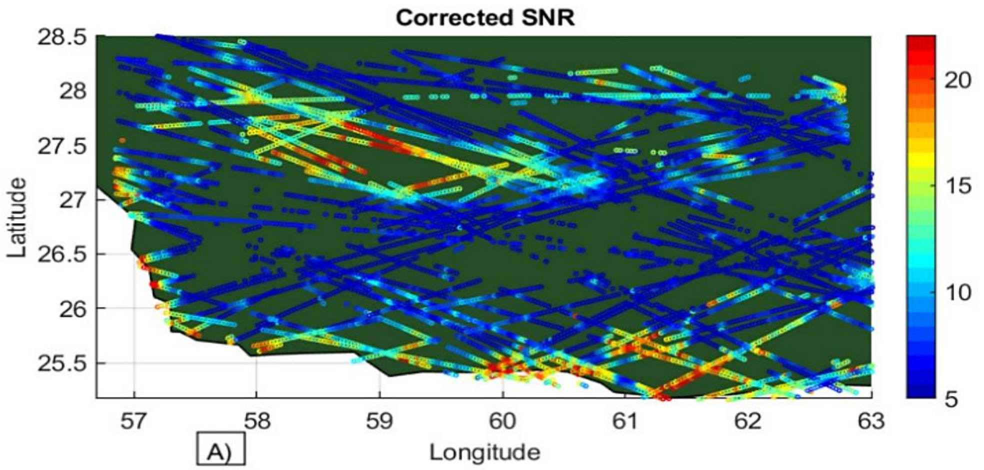

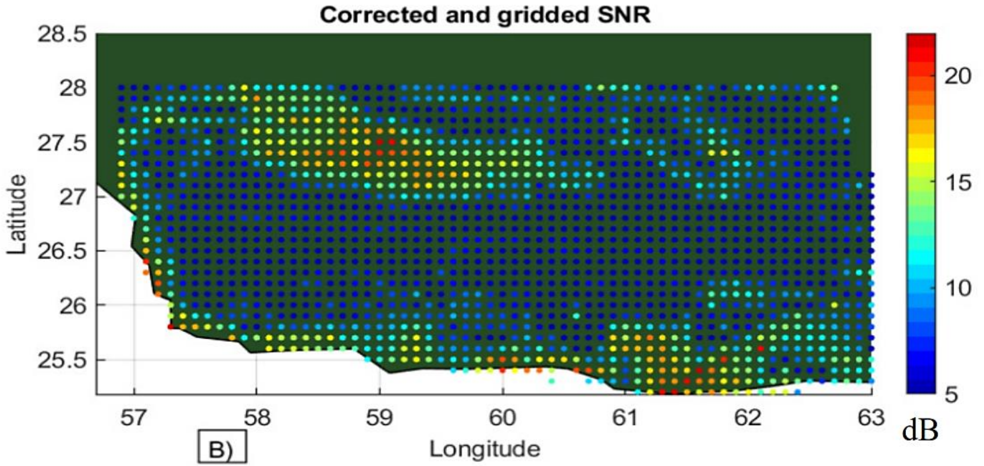

Rajabi M., Nahavandchi H., Hoseini M. (2020)

Concluding Remarks

Concluding Remarks

Concluding Remarks

Ground-based GNSS-derived tropospheric time series, a traditional data product

- **Robust homogenization** is essential for climatic applications of GNSS-derived time series

- Towards having a robust approach, we developed a novel approach that:
  - avoids miscorrection of **climate-related changes**
  - handles possible **data gaps**
  - addresses inhomogeneities **without any documentation** in stations log files

- A **significant quality improvement** was observed in an exemplary GNSS dataset over Germany after **homogenization**

Concluding Remarks

Ground-based GNSS-Reflectometry measurements, a developing data product

- Sea surface characterization results using coastal GNSS-R data show that:

  - a dedicated GNSS-R setup can make high-quality measurements of **sea level** and **sea state**

  - the measurements can reveal the **effect of the coastlines** on wind intensity

  - the **signature of rain** in GNSS-R data can be discerned under certain conditions

  - usage of dedicated **seaward antennas** enhances the quality of measurements

  - **fully polarimetric** observations can noticeably add to this enhancement

  - combination of **dual-frequency observations** increases the robustness

Concluding Remarks

Spaceborne GNSS-Reflectometry observations, a new-generation data product

- GNSS-R can observe the changes in the ocean surface roughness due to the **interaction of mesoscale ocean eddies with atmosphere**
- The observations show strong negative correlation with **surface heat flux**
- GNSS-R surface reflectivity observations can **detect flooding events** and retrieve the associated **inundated areas**

Outlook for Future Research

Outlook for Future Research

- New-generation of permanent GNSS stations with real-time GNSS-R measurements
- Spaceborne GNSS-R with multi-frequency polarimetric observations
- Addressing the issue of topography on spaceborne GNSS-R soil moisture retrieval and flood detection

Thank you for your attention!

Backup Slides

A Novel Approach based on Singular Spectrum Analysis (SSA)

Zero-Difference Homogenization

Research Approach & Results

PWV time series: $\overset{window\rightarrow}{\boxed{f_1, f_2, \dots, f_L}}, f_{L+1}, f_{L+2}, \dots, f_N$

$$\mathbf{X} = (x_{ij})_{i,j=1}^{L,K} = \begin{bmatrix} f_1 & f_2 & f_3 & \cdots & f_K \\ f_2 & f_3 & f_4 & \cdots & f_{K+1} \\ f_3 & f_4 & f_5 & \cdots & f_{K+2} \\ \vdots & \vdots & \vdots & \ddots & \vdots \\ f_L & f_{L+1} & f_{L+2} & \cdots & f_N \end{bmatrix}$$

$$\mathbf{X} = \mathbf{U}\Sigma\mathbf{V}^{\mathbf{T}}$$

$$\mathbf{X} = \mathbf{X_1} + \mathbf{X_2} + \cdots + \mathbf{X_d},\ \mathbf{X}_i = \sigma_i \mathbf{U_i}\mathbf{V_i^T}$$

$$\mathbf{X_{trend}} = \mathbf{X_1} + \mathbf{X_2} + \cdots + \mathbf{X_I}$$

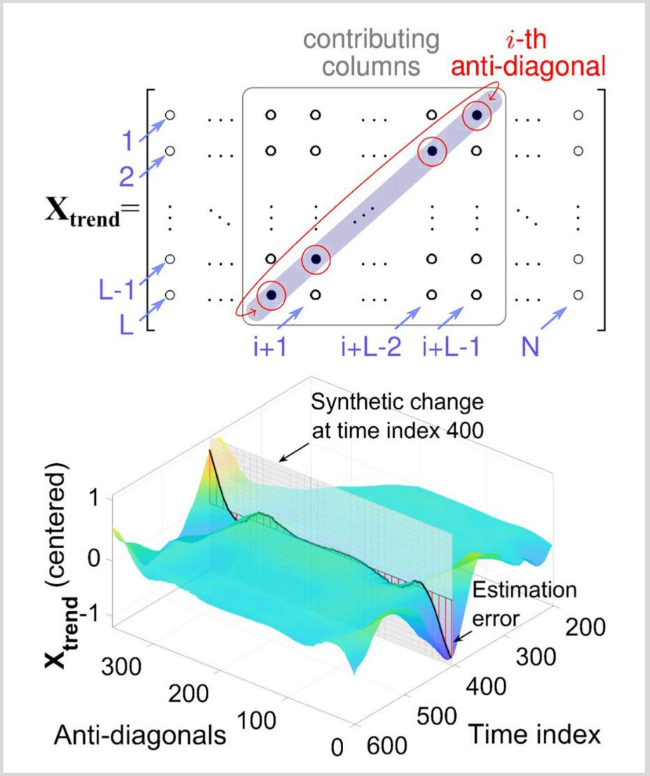

① SSA-based Change Detection

Research Approach & Results

$$\mathbf{X}_{\mathbf{trend}} = \mathbf{X}_1 + \mathbf{X}_2 + \cdots + \mathbf{X}_{\mathbf{I}} = (\hat{x}_{ij})_{i,j=1}^{L,K}$$

$$g_i = \begin{cases} \frac{1}{i} \sum_{m=1}^{i} \hat{x}_{m,i-m+1} & 1 \le i < L \\ \frac{1}{L} \sum_{m=1}^{L} \hat{x}_{m,i-m+1} & L \le i \le K \\ \frac{1}{N-i+1} \sum_{m=i-K+1}^{N-K+1} \hat{x}_{m,i-m+1} & K \le i \le N \end{cases}$$

$$\xi_i^2 = \begin{cases} 0 & i \in \{1, N\} \\ \frac{1}{i-1} \sum_{m=1}^{i} \left(\hat{x}_{m,i-m+1} - g_i\right)^2 & 1 < i < L \\ \frac{1}{L-1} \sum_{m=1}^{L} \left(\hat{x}_{m,i-m+1} - g_i\right)^2 & L \le i \le K \\ \frac{1}{N-i} \sum_{m=i-K+1}^{N-K+1} \left(\hat{x}_{m,i-m+1} - g_i\right)^2 & K < i < N \end{cases}$$

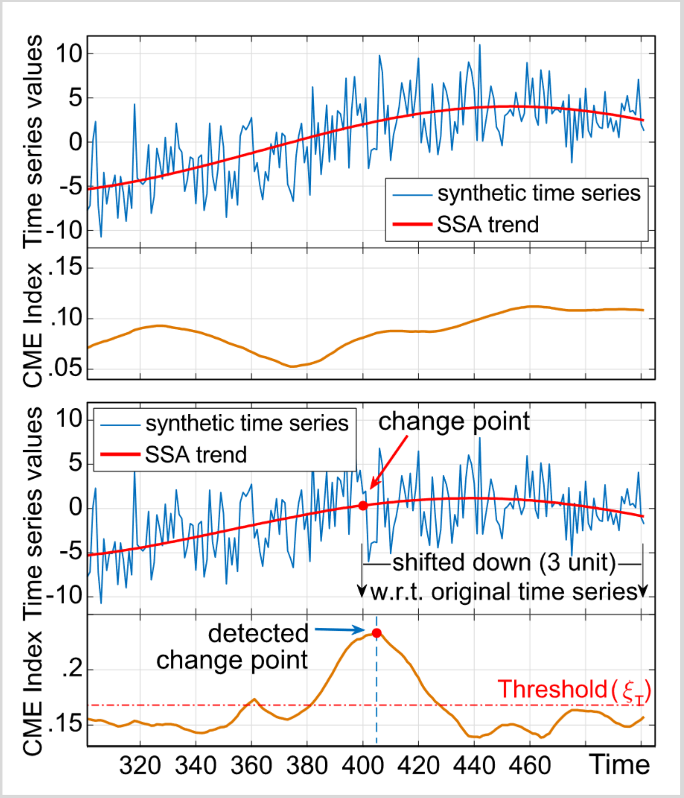

② GNSS-R Dataset Specifications

- From Jan. to Dec. **2016**
- Raw output at In-phase and Quadrature (**I/Q**) levels
- 200 Hz converted to **0.1 Hz**
- Two sea-looking antennas with **RHCP** and **LHCP** polarization
- About **3 m** above sea level

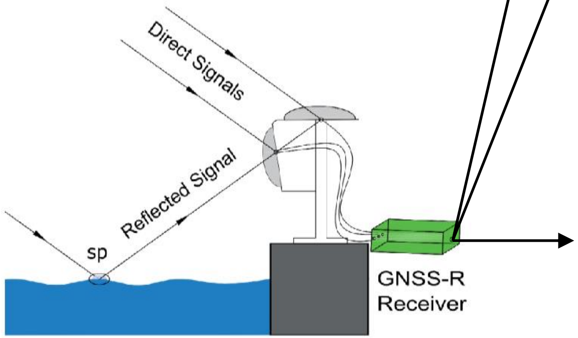

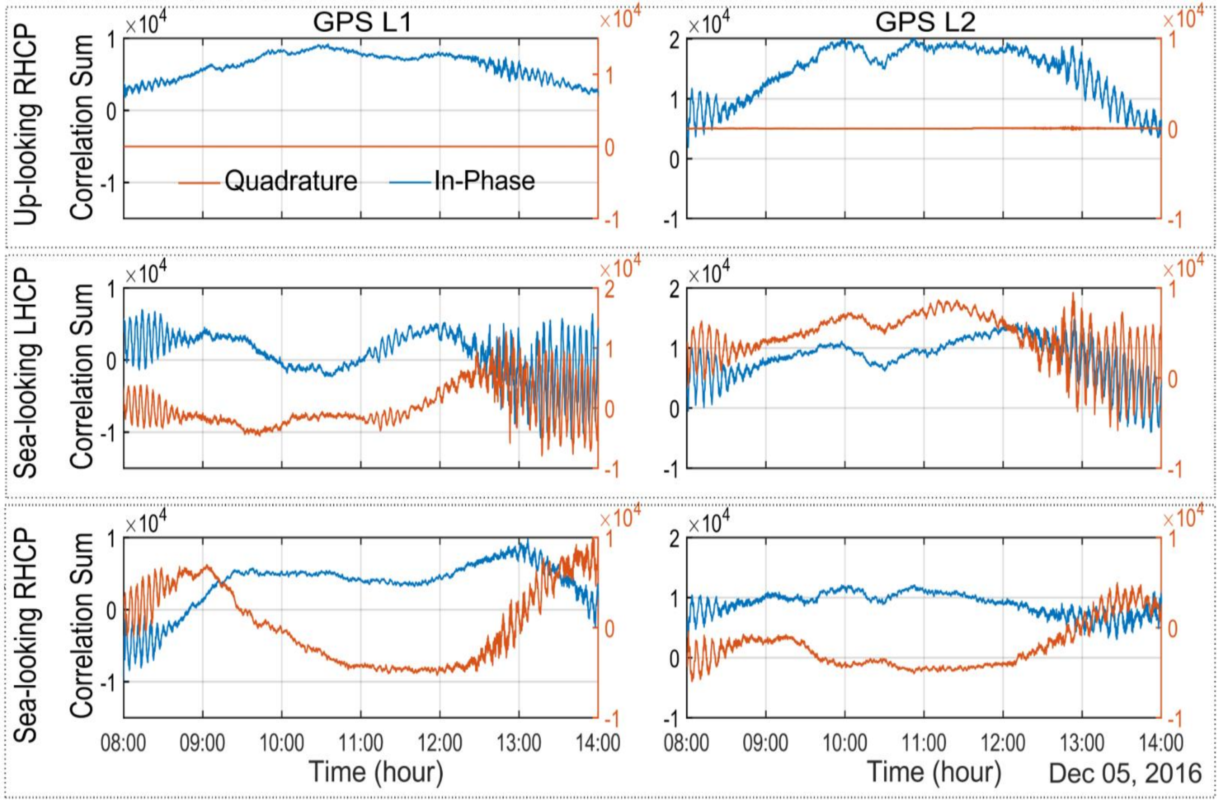

② Sea Surface Roughness

$$\hat{P}_{\text{dir}} = G_{\text{dir}}\ P_0 \qquad \hat{P}_{\text{ref}} = G_{\text{ref}}\ |R|^2\ S^2\ P_0$$

Effect of **surface roughness:** $S = \exp\left(-\frac{1}{2}\frac{(2\pi)^2}{\lambda^2}\sigma^2 \sin^2 e\right)$

co: co-polarization: (RHCP) $L^c = \frac{\hat{P}^{co}_{\text{ref}}}{\hat{P}^{co}_{\text{dir}}} = \frac{G_{\text{ref}}}{G_{\text{dir}}}\ |R^{co}|^2\ S^2$

cross: cross-polarization: (LHCP) $L^x = \frac{\hat{P}^{cross}_{\text{ref}}}{\hat{P}^{co}_{\text{dir}}} = \frac{G_{\text{ref}}}{G_{\text{dir}}}\ |R^{cross}|^2\ S^2$

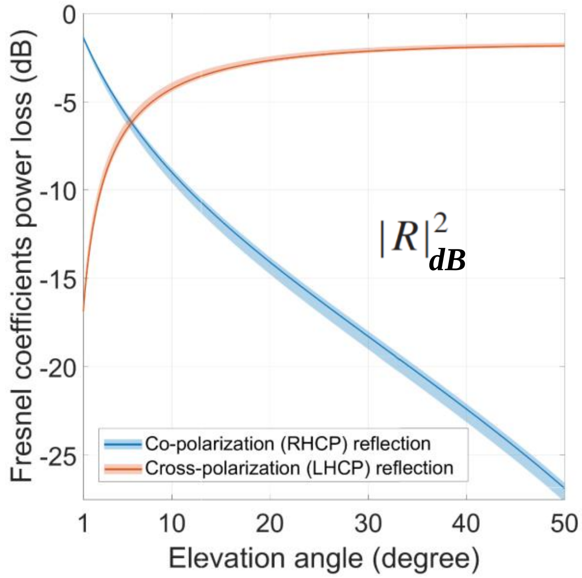

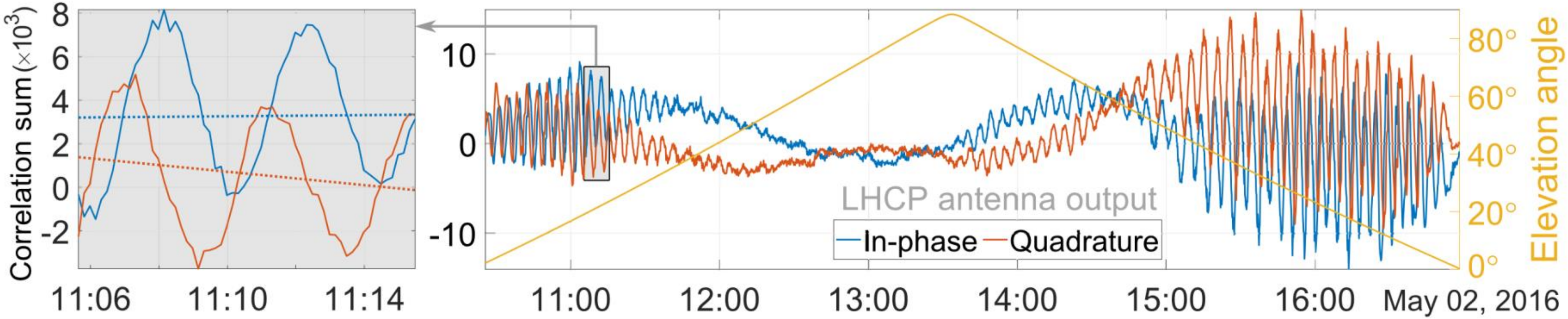

② Sea Surface Roughness

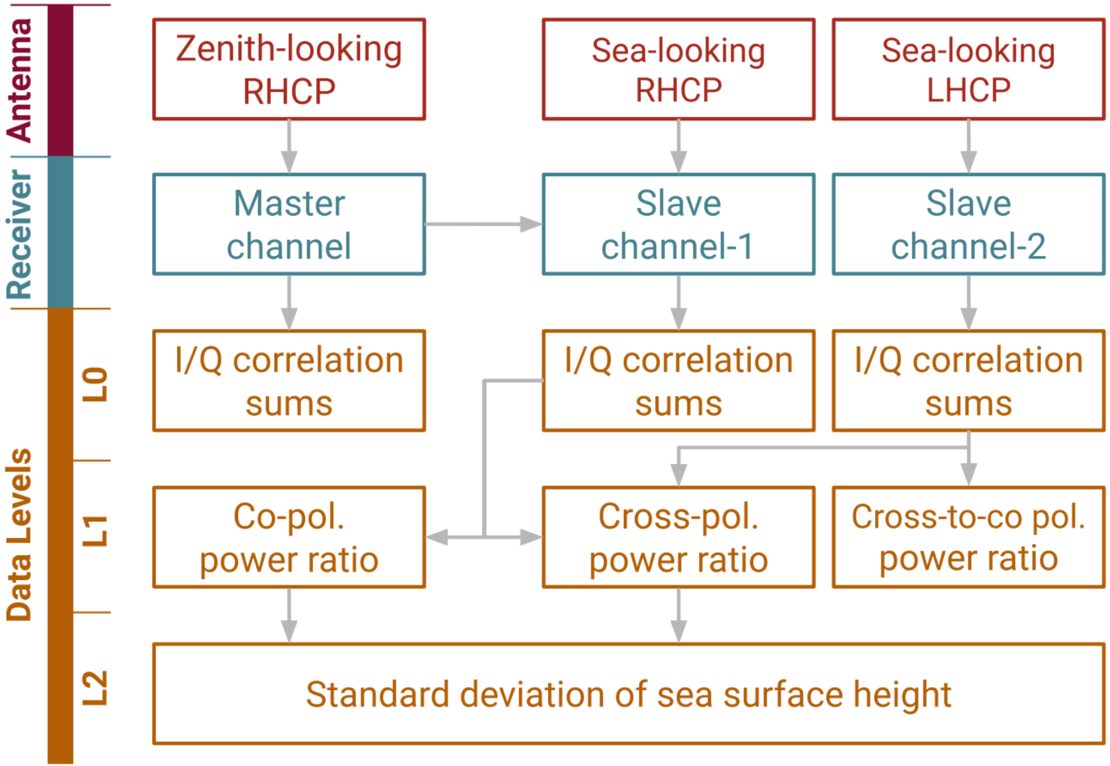

② GNSS-R Sea Level Monitoring

$$\delta f = \frac{1}{\lambda}\frac{d(\delta\rho)}{dt}, \quad \delta\rho = \rho_{\mathrm{ref}} - \rho_{\mathrm{dir}}$$

$$\delta\rho = 2\,\delta H\ \sin(e)$$

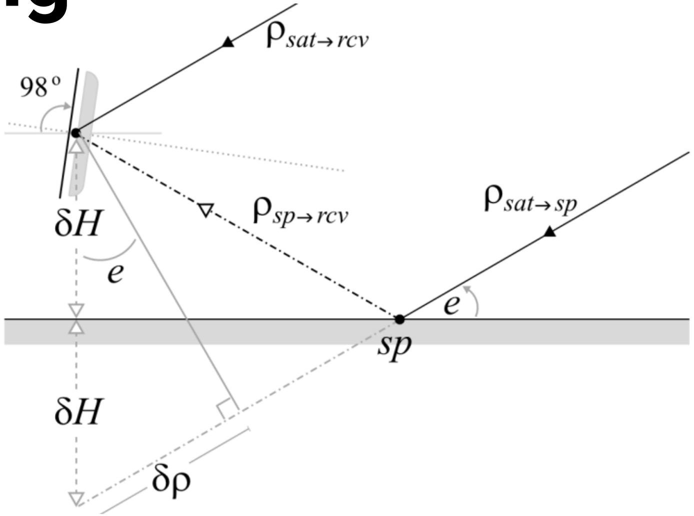

$$\delta f = \frac{2\,\delta H\ \cos(e)}{\lambda}\frac{de}{dt}$$

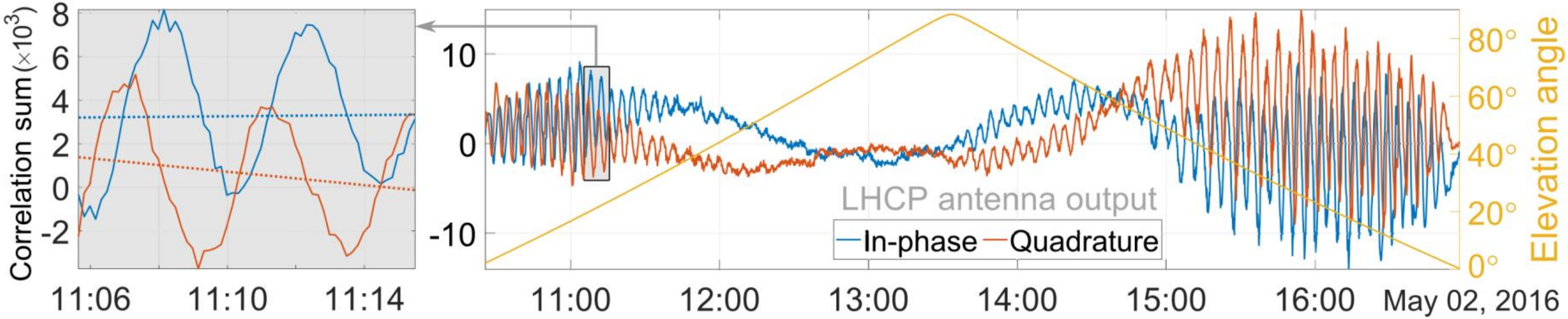

GNSS-R Response to Precipitation

An exemplary case

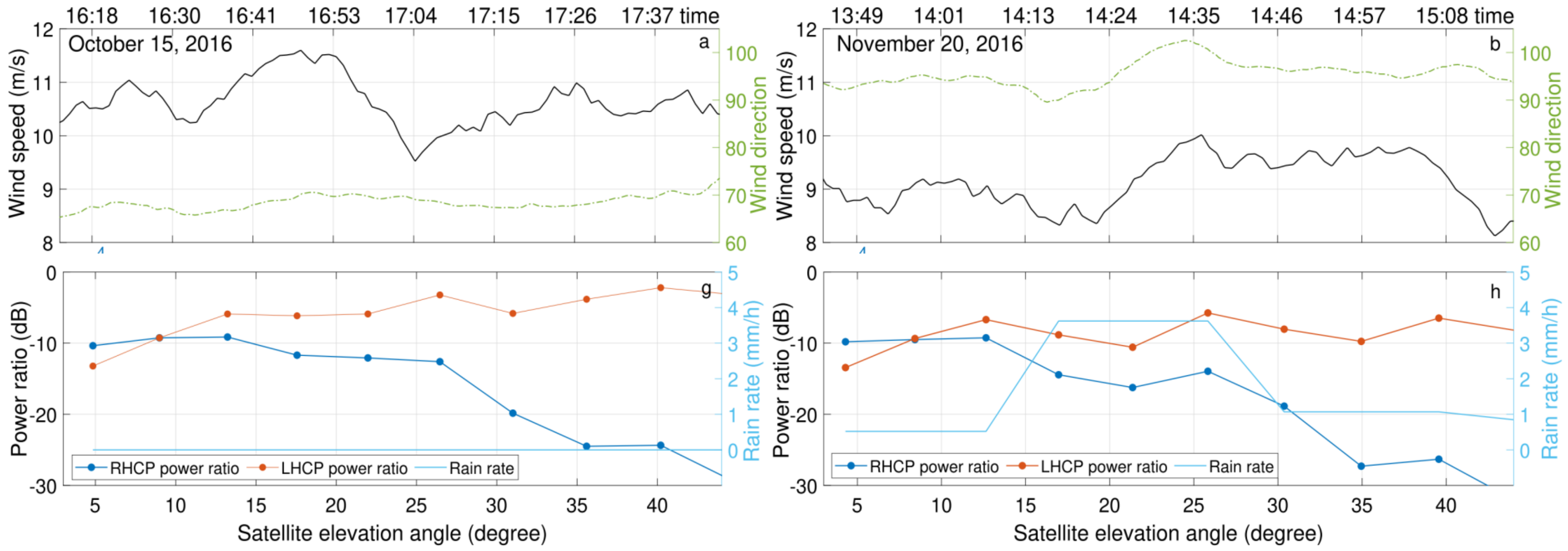

GNSS-R Sea Level Monitoring

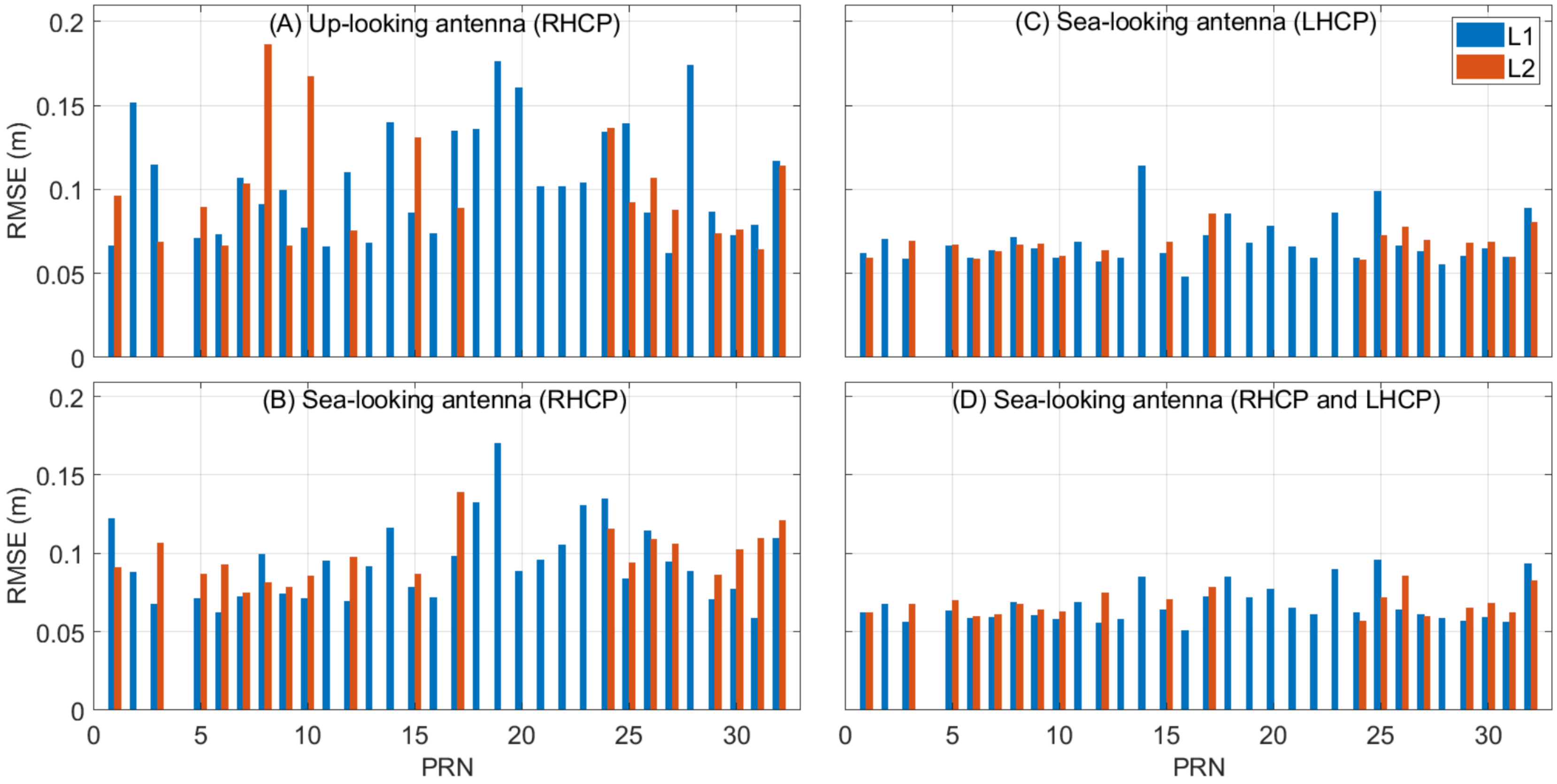

③ GNSS-R Response to the Ocean Eddies

Research Approach & Results

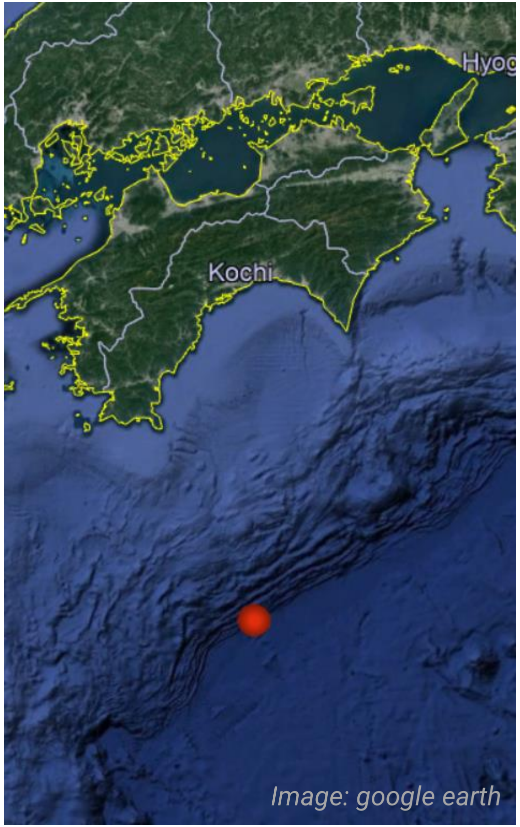

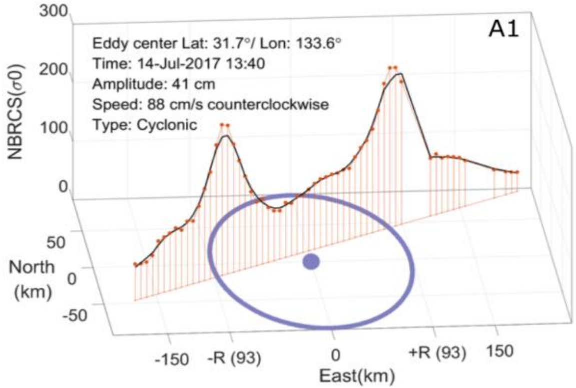

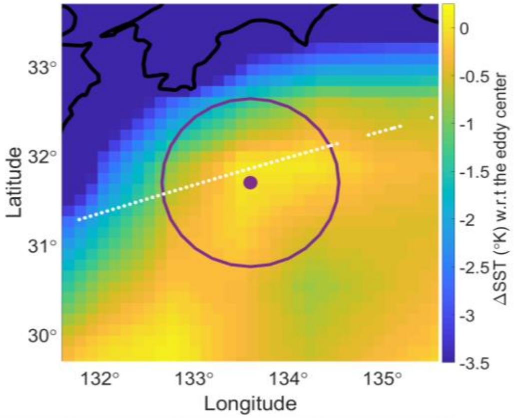

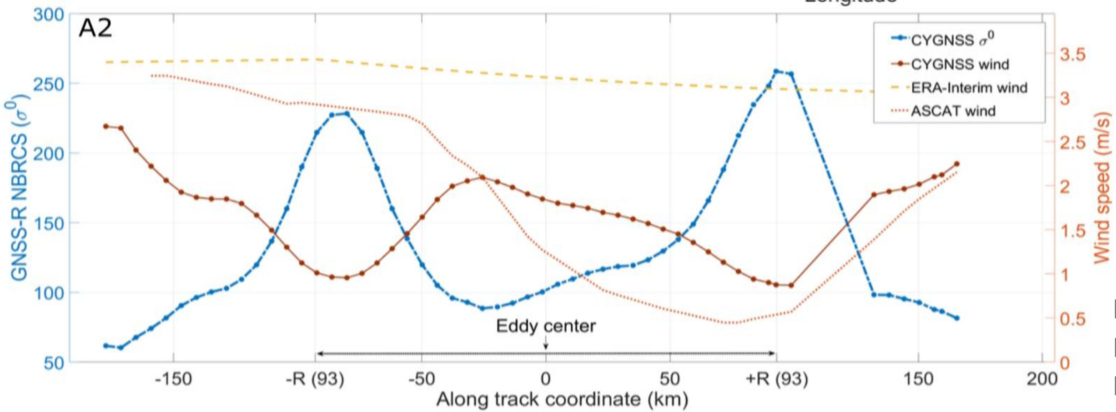

Published in IGARSS2019 Proceedings

NTNU

③ GNSS-R Response to the Ocean Eddies

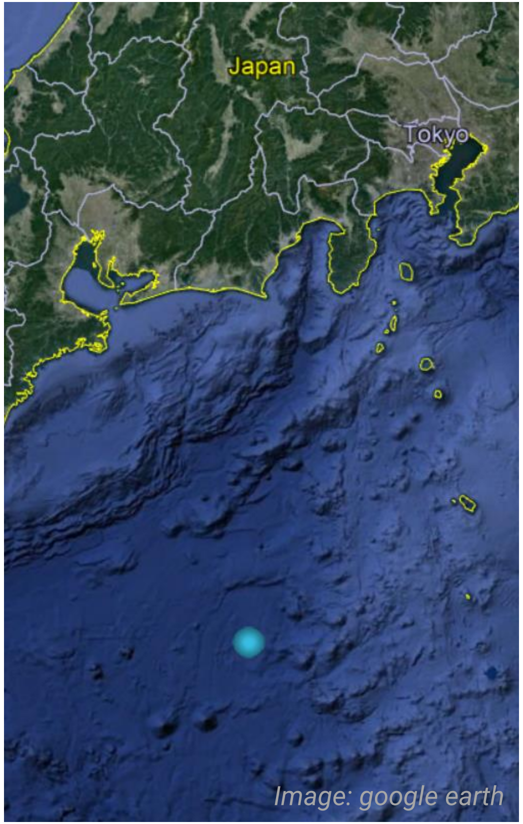

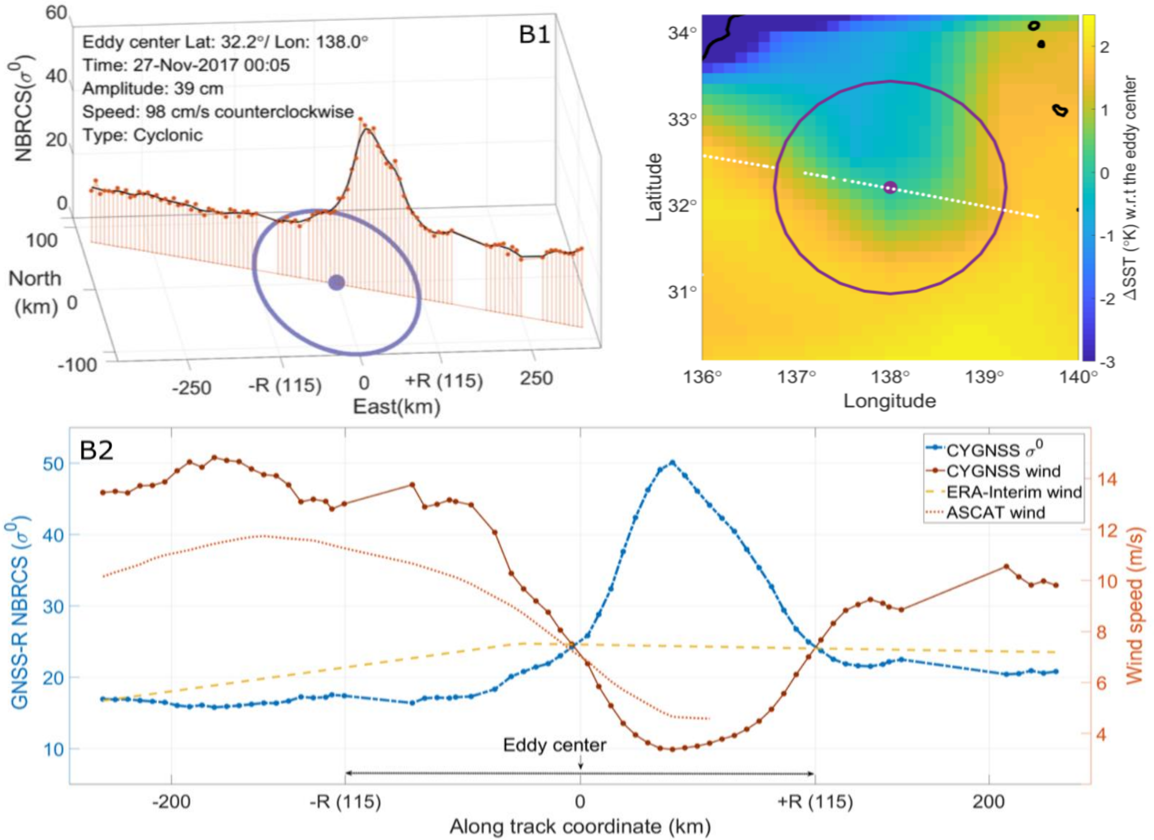

NTNU

③ Normalized Bistatic Cross Section (NBRCS)

$$P_{g,\hat{\tau},\hat{f}} = \frac{P^T \lambda^2 \bar{G}^T_{\hat{\tau},\hat{f}}\, \sigma_{0\,\hat{\tau},\hat{f}}\, \bar{G}^R_{\hat{\tau},\hat{f}} \bar{A}_{\hat{\tau},\hat{f}}}{(4\pi)^3\, (\bar{R}^T_{\hat{\tau},\hat{f}})^2\, (\bar{R}^R_{\hat{\tau},\hat{f}})^2\, \bar{L}_{a1}\, \bar{L}_{a2}}$$

$$\sigma_0(\theta) = \frac{|R(\theta)|^2}{\xi}$$

Mean Square Slope (MSS)

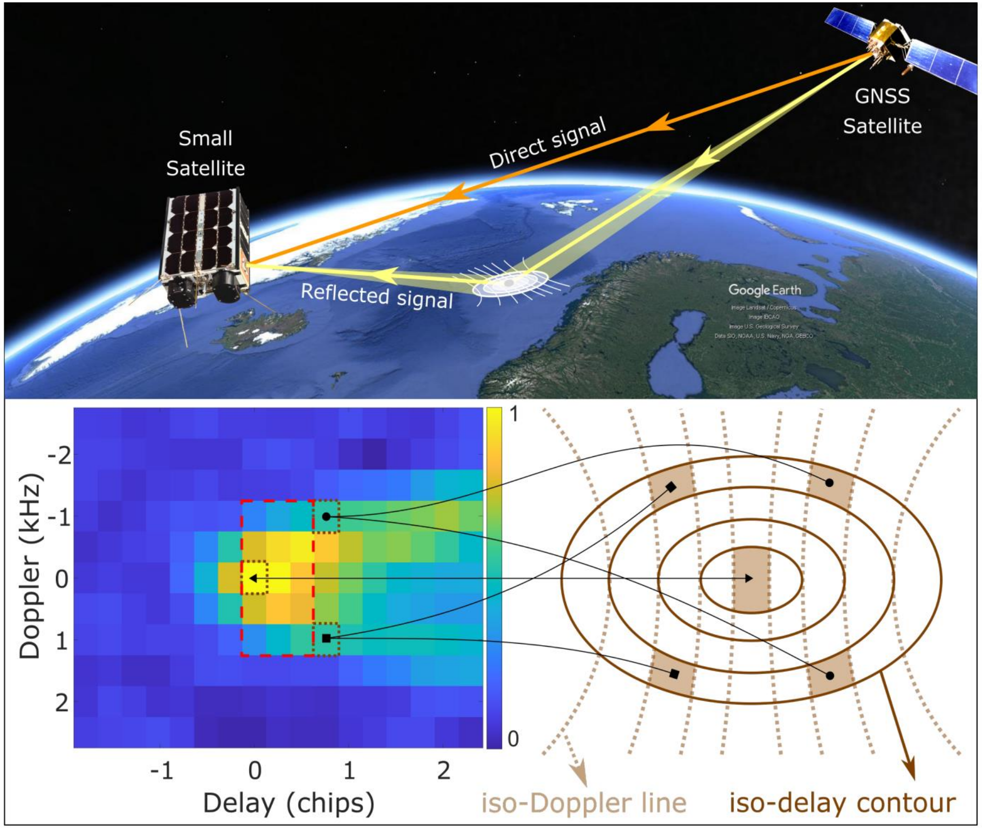

NTNU

③ Observation of Land Surface Reflectivity

$$P^R = \frac{P^T G^T}{4\pi(R^T + R^R)^2} \frac{G^R \lambda^2}{4\pi} \Gamma$$

$$P_{dB} = 10\log_{10}(P)$$

$$\Gamma_{dB} = P^R_{dB} - P^T_{dB} - G^T_{dB} - G^R_{dB} - 20\log\lambda + 20\log(R^T + R^R) + 20\log(4\pi)$$